

MODULATION EQUATIONS FOR SPATIALLY PERIODIC SYSTEMS: DERIVATION AND SOLUTIONS*

R. SCHIELEN[†] AND A. DOELMAN[‡]

Abstract. We study a class of partial differential equations in one spatial dimension, which can be seen as model equations for the analysis of pattern formation in physical systems defined on unbounded, weakly oscillating domains. We perform a linear and weakly nonlinear stability analysis for solutions that bifurcate from a basic state. The analysis depends strongly on the wavenumber p of the periodic boundary. For specific values of p , which are called resonant, some unexpected phenomena are encountered. The neutral stability curve which can be derived for the unperturbed, straight problem splits in the neighborhood of the minimum into two, which indicates that there are *two* amplitudes involved in the bifurcating solutions, each one related to one of the minima. The character of the modulation equation, which describes the nonlinear evolution of perturbations of the basic state, depends crucially on the distance of the bifurcation parameter from the lowest, most critical minimum. In a relatively large part of the parameter space, we derive a coupled system of amplitude equations. This can either be reduced to an equation for a *real* amplitude with cubic and quadratic terms or it can be written as a Ginzburg–Landau equation for a *complex* amplitude A , with an additional term, proportional to \bar{A} . For this latter equation, we study the existence and stability of periodic solutions. We find that the nonsymmetric term \bar{A} decreases the width of the Eckhaus band of stable solutions. Numerical simulations show that complex periodic solutions bifurcate into stable, real solutions for increasing influence of the \bar{A} -term.

Key words. Ginzburg–Landau equation, pattern formation, nonlinear stability analysis

AMS subject classifications. 35A99, 35Q35, 35R99, 58Gxx, 65C99, 76E30

PII. S003613999630318X

1. Introduction. In the classical analysis of nonlinear stability problems defined on unbounded domains, one usually assumes a simple geometry of the domain in the unbounded direction. The problem is often formulated on a cylindrical domain $\Omega \times \mathbf{R}^n$, where $\Omega \subset \mathbf{R}^p$ is bounded (and $n = 1$ in most cases; see [7] for a review). However, this assumption is not satisfied in a realistic physical system: boundaries of experimental set-ups (such as flumes, annuli, parallel plates) are never perfectly straight but show, of course, imperfections in their geometry. To a greater extent, the same is true for realistic physical situations in the field. The motivation for the analysis presented in this paper comes actually from the problem of determining the bottom formation in perfectly straight channels with an erodible bottom and nonerodible side-walls (see [15]). As a natural next step, one would like to consider again the problem of bottom formation, but in a *slightly meandering* channel (with erodible bottom and nonerodible side-walls); hence, one considers the model on a domain which is periodic in the unbounded direction. There are more examples of physical systems which are defined and studied on not purely cylindrical domains: Bénard convection [4], [20], convection in a porous layer [10], [11], [12], [13], and Taylor vortex flows [5].

In what follows, we will assume that the boundaries of the domains can be modelled by small amplitude, p -periodic functions. A difficult element in the analysis of

*Received by the editors May 8, 1996; accepted for publication (in revised form) June 11, 1997; published electronically August 18, 1998.

<http://www.siam.org/journals/siap/58-6/30318.html>

[†]Delft Hydraulics, P.O. Box 152, 8300 AD Emmeloord, the Netherlands. Present address: IMN Nederland, P.O. Box 688, 3700 AR Zeist, the Netherlands (r.schielen@imn.nl).

[‡]Department of Mathematics, Utrecht University, P.O. Box 80.010, 3508 TA, the Netherlands (doelman@math.ruu.nl).

these problems is the treatment of the boundary conditions in relation to the periodic geometry on which the problem is defined. To deal with these problems, one can do the following. We distinguish between the physical (x, y) -domain (on which the problem with the p -periodic boundaries “lives”) and the computational (s, n) -domain (here, x and s represent the unbounded directions and y and n the bounded directions). The computational domain is the “straightened” physical domain. The straightening is accomplished by a transformation T which relates the (x, y) -coordinates to the (s, n) -coordinates. T contains small amplitude, periodic terms, which reflects the fact that the boundaries are not perfectly straight but are instead slightly oscillating. The “slightness” is reflected by the introduction of a small parameter ν . We use T to transform the model for some physical situation, which we write down in a general fashion as

$$(1.1) \quad \frac{\partial \Phi}{\partial t} = L_R \Phi + N(\Phi)$$

for a vector of unknowns Φ , depending on a spatial coordinate $x \in \mathbf{R}$ and on time t , a linear operator L_R , depending on a bifurcation parameter R and a nonlinear operator N . The bifurcation (or control) parameter R is related to the Rayleigh number in convection models and to the width/depth ratio of the river in the river bed problem (see [15]). The reason that we take x to be one-dimensional and that we neglect the transverse direction is only for simplicity: dropping these assumptions will merely cause technical complications but will not reveal new phenomena. Apart from x and y , which are transformed into s and n using T , the *derivatives* with respect to x and y must also be transformed into derivatives with respect to s and n . Due to the fact that T contains small periodic terms, the transformed derivatives also contain these terms. Hence, on the straightened, computational domain, (1.1) reads

$$(1.2) \quad \frac{\partial \Phi}{\partial t} = \tilde{L}_R \Phi + \tilde{N}(\Phi),$$

where Φ now depends on s and n and where \tilde{L}_R and \tilde{N} have $O(\nu)$ variable coefficients generated by T .

The aim of the nonlinear stability analysis is then to find a simple basic state which represents some realistic physical situation and consider the stability properties of that basic state. Finding a basic state for the “straight” problem (i.e., $\nu \equiv 0$) is almost always trivial. However, in general it is not possible to find an explicit form for a basic state of (1.2). On the other hand, we can use the small parameter ν to express the basic state in an asymptotic series in ν . We assume that this basic state is given by $\phi(\nu)$. The stability properties of this solution can be analyzed by considering

$$(1.3) \quad \Phi = \phi(\nu) + \Psi.$$

By construction, $\Phi = \phi(\nu)$ (i.e., $\Psi = 0$) will be a solution of (1.2), and stability properties of $\Psi = 0$ are directly related to the stability properties of $\phi(\nu)$. Then we expand the operators \tilde{L}_R and \tilde{N} also in ν (which involves again $O(\nu)$ periodic terms), substitute (1.3) in (1.2), and derive a partial differential equation for Ψ . In its most simple form (which means that, among other assumptions, we neglected the y -dependence and $O(\nu^2)$ -terms), this equation reads

$$(1.4) \quad \frac{\partial \Psi}{\partial t} = \mathcal{L}_R \Psi + \nu f(px) \Psi + \mathcal{N}(\Psi) \quad \text{with} \quad \mathcal{N}(\Psi) = \mathcal{P}(\Psi) \mathcal{Q}(\Psi),$$

where $\Psi = \Psi(x, t)$ with $x \in \mathbf{R}$, \mathcal{L}_R , \mathcal{P} , and \mathcal{Q} are linear operators in $\frac{\partial}{\partial x}$ and R is again the control parameter. Note that we reintroduced x instead of s . The slightly varying geometry is modelled by a p -periodic “forcing term” $\nu f(px)$, with $0 < \nu \ll 1$. It will be convenient to write f as a Fourier series:

$$(1.5) \quad f(px) = \sum_{n=-\infty}^{\infty} F_n e^{inpx}$$

with $F_n \in \mathbf{C}$ and $F_{-n} = \bar{F}_n$, since $f(px) \in \mathbf{R}$. The period p of f will be determined by external conditions and is considered to be $O(1)$ and fixed. We assume that $F_0 = 0$, which means that f has 0-average. This is, of course, no limitation because a nonzero average term F_0 has the same influence on (1.4) as an $O(\nu)$ shift in the control parameter R . By setting $F_0 = 0$ we know that influence of f on the system is purely due to its periodicity. Note that we made some additional simplifying assumptions: the nonlinear operator $\mathcal{N}(\Psi)$ consists of only one quadratic term and the periodic term νf only appears in the linear part of (1.4). These assumptions only reduce the amount of the computations; more general terms will not create new phenomena. We will use (1.4) as a model problem to understand the influence of a slightly varying geometry on the nonlinear stability problem. The simplicity of this model enables us to focus fully on the sometimes subtle effects of the periodic terms. We believe that the one-dimensional model exhibits, in essence, all aspects of pattern formation in systems on periodically modulated domains. In other words, in more realistic problems with transverse dimensions the complications will be merely technical, but the modulation equations will be similar to the equations derived in this paper for the model problem.

We summarize very briefly the linear and weakly nonlinear stability analysis for the solution $\Psi = 0$ of (1.4) for $\nu \equiv 0$. One substitutes $\Psi = \varepsilon \exp(ikx + \omega t)$, $\varepsilon \ll 1$, and finds after linearization $\omega(k, R) = \mu(k, R)$, with μ the symbol of the operator \mathcal{L}_R (the symbol μ is defined by $\mathcal{L}_R(\exp(ikx)) = \mu(k, R)\exp(ikx)$). Now we make an additional assumption: we assume that there is an $x \rightarrow -x$ reflection symmetry present in \mathcal{L}_R . As a consequence, μ is real. Furthermore, we assume that the structure of \mathcal{L}_R is such that the neutral stability curve $\omega = 0$ has a minimum for $R = R_c^o, k = k_c^o$; besides $\omega < 0$ for $R < R_c^o$. Hence, the wave $\exp(ik_c^o x)$ is the first wave to become unstable for increasing R , starting below R_c^o . Continuing the analysis with weakly nonlinear theory, we consider values of the bifurcation parameter close to criticality ($R = R_c^o + r\varepsilon^2$) and apply a weakly nonlinear stability theory to consider the nonlinear evolution of small perturbations of $\Psi = 0$. By now it is well known that the spatial and temporal evolution of these perturbations is governed by the Ginzburg–Landau equation, a modulation equation for the amplitude $A(\xi, \tau)$ (which depends on rescaled spatial and temporal coordinates). This amplitude modulates the linear most unstable wave $\exp(ik_c^o x)$. The asymptotic validity of this equation has been shown in [19].

We summarize some important conclusions of this paper. First of all, we will see that, for p (the period of f in (1.4)) such that $Np/2$ is “close” to k_c^o for some arbitrary but fixed integer N , some unexpected phenomena in the linearized theory appear. We will call these values of p *resonant*. The most striking result is that the neutral stability curve splits into two, which means that there are two critical values for the bifurcation parameter R : R^+ and R^- , with $R^+ < R^-$ and $|R^+ - R^-| = O(\nu)$. This means that the first bifurcation occurs at R^+ and a second one occurs at R^- . The nonresonant values of p turn out to be not very interesting, in the sense that the results that one finds for the case $\nu \equiv 0$ are “regularly perturbed.” This means, for

the nonlinear theory, that we find essentially the same results as in the case $\nu \equiv 0$, with $o(1)$ corrections in the coefficients of the Ginzburg–Landau equation. This case is analyzed in detail in [14].

The results for the resonant values of p depend strongly on the relative magnitudes of ε and ν , where $\varepsilon = O(\sqrt{R - R^+})$, i.e., ε measures the distance of the bifurcation parameter R to criticality. The area of interest is essentially divided into four parts: $0 \ll \varepsilon \ll \nu^2, \nu^2 \ll \varepsilon \ll \sqrt{\nu}, \varepsilon = O_s(\sqrt{\nu})$, and $\varepsilon \gg \sqrt{\nu}$. In the first part, R^- is relatively so *far away* from R^+ that the nonlinear analysis, which is performed in an ε -neighborhood of R^+ , does not “feel” the influence of R^- . If $\varepsilon \gg \sqrt{\nu}$, both critical conditions R^+ and R^- are relatively *so close* to each other that they can be identified. In both cases, the usual nonlinear theory can be applied, be it with some minor changes. This is to say that one can derive a Ginzburg–Landau equation which describes the nonlinear evolution of the linearly most unstable wave. However, it turns out that this linearly most unstable wave (i.e., the equivalent of the single Fourier mode $\exp(ik_c^o x)$ for $\nu \equiv 0$) has now a more complicated (sometimes quasi-periodic) structure. This is again due to the periodic term f in (1.4).

In the parameter regime $\nu^2 \ll \varepsilon \ll \sqrt{\nu}$ we must take explicitly into account that there occur two bifurcations, one at R^+ and one at R^- . This is reflected by the fact that the structure of the bifurcating waves involve two amplitudes, B^+ and B^- , which are, however, essentially real. This is to say that $B^+ \in l^+, B^- \in l^-$, where l^+ and l^- are orthogonal lines in the complex plane. A special case is encountered when l^+ coincides with the real axis: then $B^+ \in \mathbf{R}$ and $B^- \in i\mathbf{R}$. The nonlinear analysis then leads to a coupled system of amplitude equations:

$$(1.6) \quad B_\tau^+ = r^+ \omega_R^+ B^+ - \frac{1}{2} \omega_{kk}^+ B_{\xi\xi}^+ + \beta B^+ ((B^+)^2 \psi_N^+ + (B^-)^2 \psi_N^-),$$

$$(1.7) \quad B_\tau^- = (r^+ - \delta) \omega_R^- B^- - \frac{1}{2} \omega_{kk}^- B_{\xi\xi}^- + \beta B^- ((B^+)^2 \psi_N^+ + (B^-)^2 \psi_N^-),$$

where $R - R^+ = r^+ \varepsilon^2$ and $\delta = (R^- - R^+)/\varepsilon^2 = O(\nu/\varepsilon^2)$. The other coefficients in (1.6)–(1.7) are not important at this moment. What *is* important is that, for $\varepsilon \ll \sqrt{\nu}$, the linear coefficient in (1.7) causes exponential damping of B^- . Hence, there remains only the equation for B^+ (in which $B^- = 0$) which is a Ginzburg–Landau equation for the *real* amplitude B^+ . For $\varepsilon = O_s(\sqrt{\nu})$, (1.6)–(1.7) can be combined into one equation for a *complex* amplitude A defined as $A = B^+ + B^-$ (naturally, B^+ plays the role of the real part, B^- plays the role of the imaginary part):

$$(1.8) \quad A_\tau = \hat{r} \omega_R A - \frac{1}{2} \omega_{kk} A_{\xi\xi} + \beta |A|^2 A + \frac{1}{2} \delta \omega_R \bar{A}.$$

Again, the meaning of the coefficients is not important at this moment. In what follows, we will refer to this equation as the *nonsymmetric Ginzburg–Landau equation*. The nonsymmetric part is formed by a term proportional to \bar{A} . The influence of this term vanishes as $\nu \rightarrow 0$ (because $\delta = O(\nu/\varepsilon^2)$), and we are left with the usual Ginzburg–Landau equation, as to be expected.

In this paper, we will analyze in detail the linear analysis of the model problem (1.4) and focus on the weakly nonlinear analysis for ε between ν^2 and $\sqrt{\nu}$. This is the most interesting part of the $\varepsilon - \nu$ -parameter space. In the analysis of (1.8), we focus on the influence of the \bar{A} -term on the Eckhaus stability criterion (which states that there is a band of nonlinearly stable, periodic solutions of the “usual” Ginzburg–Landau equation (without the \bar{A} -term); see [6]). Considering the $O(\delta)$ -term in (1.8)

as a small perturbation of the usual Ginzburg–Landau equation, it may be anticipated that the Eckhaus band gets a $O(\delta)$ -adaption. In order to see whether it increases or decreases, a stability analysis of solutions of (1.8) is performed and the conclusion is that the Eckhaus band becomes narrower. Hence, the small periodic fluctuation of the boundary in the model problem not only has a destabilizing effect on the linear theory, but also on the nonlinear theory. Numerical simulations of solutions of (1.8), in which we allow the nonsymmetric part to become $O(1)$, acknowledge that in a specific part of the $\varepsilon - \nu$ -parameter space these solutions become real. This result is already obtained with low-dimensional spectral models, with only seven complex modes.

The organization of this paper is as follows. In the next section, we consider the linear theory of the model problem and focus our attention on the splitting of the neutral stability curve for resonant values of p . In section 3, we describe the structure on the linearly most unstable waves, which form the starting point of section 4: the derivation of the amplitude equations for resonant p and for the different regimes in the $\varepsilon - \nu$ -parameter space. In section 5, we analyze spectral solutions of the nonsymmetric Ginzburg–Landau equation (with a small nonsymmetric term), and in section 6, we perform some numerical simulations of that equation, in which we allow the nonsymmetric part to become $O(1)$.

Remark. In this paper we focus on the case in which the period p of the spatial structure of the domain is $O(1)$. The case $p = o(1)$, i.e., a slightly *and slowly* varying domain, has been considered in [8]. The relation between the approach of this paper and that of [8] has been discussed in [2].

2. Linear theory for the model problem. In this section, we perform the linear stability theory for the model problem (1.4). This will lead to a reinterpretation of the neutral stability curve as it is encountered in the previous section (i.e., $\omega(k, R) = \mu(k, R) = 0$, with μ the symbol of \mathcal{L}_R).

We perturb the basic state $\Psi = 0$ (which also satisfies (1.4) for $\nu \neq 0$) and look at the linear stability properties of the perturbation. Due to the structure of the small periodic term $\nu \sum F_l e^{ilpx}$, the perturbation must be of the following quasi-periodic structure:

$$(2.1) \quad \Psi = \varepsilon \psi_{lin} = \varepsilon e^{ikx + \omega t} \sum \psi_l(k, R) e^{ilpx} + \text{c.c.},$$

where c.c. means complex conjugated, k is an arbitrary wave number, and ω is again the growth rate of the waves. Summation is always taken over l , unless specified otherwise. As usual, the sign of the real part of ω determines the stability properties of the perturbation (2.1). Due to the structure of ψ_{lin} , we have to be careful about the interpretation of the set $\omega = 0$ in the (k, R) -plane. As a result of the periodic function f in the model problem, the outcome of the linear theory will be periodic in k . To see this, we consider (2.1) for $k = \tilde{k} + Np, N \in \mathbb{N}$, and observe

$$(2.2) \quad \begin{aligned} \psi_{lin} &= e^{i(\tilde{k} + Np)x + \omega t} \sum \psi_l(\tilde{k} + Np, R) e^{ilpx} + \text{c.c.} \\ &= e^{i\tilde{k}x + \omega t} \sum \psi_l(\tilde{k} + Np, R) e^{i(l+N)p x} + \text{c.c.} \\ &= e^{i\tilde{k}x + \omega t} \sum \psi_{l-N}(\tilde{k} + Np, R) e^{ilpx} + \text{c.c.} \\ &= e^{i\tilde{k}x + \omega t} \sum \tilde{\psi}_l(\tilde{k}, R) e^{ilpx} + \text{c.c.}, \text{ with } \tilde{\psi}_l(\tilde{k}, R) = \psi_{l-N}(\tilde{k} + Np, R). \end{aligned}$$

Thus, we can study the perturbations given in (2.1) for k limited to an interval with length p ; the results we obtain are p -periodic, and therefore $\omega(k, R) = \omega(k + Np, R)$.

Geometrically this means that the unperturbed ($\nu \equiv 0$) graph of $\omega = \mu(k, R)$ should now be interpreted on a cylinder. This observation gets a more natural meaning in the sequel of the analysis, when we observe that we get degenerate situations in the neighborhood of intersections of $\mu(k, R)$ and $\mu(k + Np, R)$. With the interpretation on the cylinder, these intersections can then be regarded as self-intersections of $\mu(k, R)$.

Substitution of (2.1) (where we have scaled $\psi_0 \equiv 1$) into the model problem (1.4) and linearizing the results yield an equation for every coefficient ψ_l of the Fourier series (2.1). For $l = 0$, we find a formula for the growth rate ω , which is an $o(1)$ correction of the growth rate as can be found for the case $\nu \equiv 0$:

$$(2.3) \quad \omega(k, R) = \mu(k, R) + \nu \sum_{s+t=0} F_s \psi_t.$$

For $l \neq 0$ we find equations for the coefficients ψ_l , recursively defined

$$(2.4) \quad \psi_l = \nu \frac{\sum_{s+t=l} F_s \psi_t}{\omega(k, R) - \mu(k + lp, R)}.$$

Thus, for $|\omega(k, R) - \mu(k + lp, R)| = O(1)$, we see that $\psi_l = O(\nu), l \neq 0$, and since $\psi_0 = 1$, setting the index $t = 0$ in (2.4) yields the leading-order term of $\psi_l, l \neq 0$:

$$(2.5) \quad \psi_l = \nu \frac{F_l}{\mu(k, R) - \mu(k + lp, R)}$$

(here, we have also used (2.3)). Substitution of (2.5) into (2.3) gives an explicit expression for the $O(\nu^2)$ correction on $\omega(k, R)$ in the perturbed case:

$$(2.6) \quad \omega(k, R) = \mu(k, R) - \nu^2 \sum \frac{|F_l|^2}{\mu(k + lp, R) - \mu(k, R)} + O(\nu^3).$$

We expect degenerate situations with respect to the magnitude of $|\omega - \mu|$ whenever $|\omega(k, R) - \mu(k + Np, R)| = o(1)$ for some $N \in \mathbf{Z} - \{0\}$.

The magnitude of $|\omega - \mu|$ is of particular importance when we consider the situation near the unperturbed critical conditions $k = k_c^o, R = R_c^o$, since the subsequent nonlinear stability theory is performed near the “new” critical conditions (they will be defined later on, but they are expected to be in the neighborhood of $k = k_c^o, R = R_c^o$). In [14], the analysis is given for general k ; here we focus on the analysis for (k, R) near (k_c^o, R_c^o) . Because μ is symmetric in k , we expect degenerations if there exists an N such that

$$(2.7) \quad p = -\frac{2k_c^o}{N} + o(1).$$

Relation (2.7) is called the *resonance condition*.

In order to perform a weakly nonlinear stability analysis, it is important to derive the neutral stability curve, given by $\omega = 0$. The minimum of this curve plays a vital role in the nonlinear analysis.

In what follows we will show that, for $|\mu(k + Np, R) - \mu(k, R)| = o(1)$ (which can be regarded as self-intersections of the curve $\mu(k, R)$ on the cylinder), the curve $\omega(k, R)$ splits into two, ω^u and ω^l , which are $O(\nu)$ close together. For *nonresonant* values of p , the splitting phenomenon is not relevant; the new critical conditions $(k_c(\nu), R_c(\nu))$,

i.e., the minimum of $\omega = 0$, are $O(\nu^2)$ close to (k_c^o, R_c^o) . The correction on R_c^o is strictly negative, and thus, introducing a periodic variation into the geometry of the problem has a destabilizing effect. Things become interesting for resonant values of p because then the splitting occurs in the neighborhood of k_c^o . The result is that we should take into account *two* neutral stability curves, defined as ω^+ and ω^- .

At many points in the analysis, the theory should be divided into two: a resonant part and a nonresonant part. However, it turns out that the nonresonant theory is not of particular interest. The results for the unperturbed problem get an $o(1)$ correction, and qualitatively, the situation does not change. The resonant problem is more interesting, and in the rest of this paper we will focus on the latter problem.

The splitting phenomenon is one of the most striking results of the linear analysis. It can be understood by analyzing $\omega(k, R)$ near an intersection of $\mu(k, R)$ and $\mu(k + Np, R)$ for a certain $N \in \mathbf{Z}$. Therefore, we introduce the unknowns S and α by

$$(2.8) \quad \omega(k, R) = \alpha(k, R) + S\nu^\alpha + \text{h.o.t.}$$

and consider a situation in which

$$(2.9) \quad \mu(k + Np, R) - \mu(k, R) = Q\nu^\lambda, \quad \lambda > 1 \text{ certain } Q.$$

Substitution of (2.9) and (2.8) into (2.3) and (2.4) gives, after some calculations,

$$(2.10) \quad S\nu^\alpha = -\nu^2 \frac{|F_N|^2}{Q\nu^\lambda - S\nu^\alpha} + O(\nu^2).$$

Suppose that $\lambda > \alpha$. Then, it is clear from (2.10) that $S_{1,2} = \pm|F_N|$ and $\alpha = 1$. This means that there are *two* corrections on ω , the already mentioned curves ω^+ and ω^- :

$$(2.11) \quad \omega(k, R) = \omega^\pm(k, R) = \mu(k, R) \pm \nu|F_N| + \text{h.o.t.} \quad \text{for } \lambda > 1.$$

The two remaining cases, $\lambda = 1$ and $\lambda < 1$, show that there is a smooth transition from the $O(\nu^2)$ correction of ω sufficiently far away from the intersection of $\mu(k, R)$ and $\mu(k + Np, R)$, toward the $O(\nu)$ correction described above (see [14]). This “splitting” phenomenon is sketched in Figure 2.1. The set $\omega(k, R)$ is a collection of curves “near” $\mu(k, R)$ and—by the periodicity—near $\mu(k + Np, R)$. We see that different branches of ω cannot intersect—unlike the branches of μ on the cylinder. The two branches of the neutral set, $\omega^+(k, R) = 0$ and $\omega^-(k, R) = 0$, are almost everywhere $O(\nu^2)$ near the unperturbed neutral curve $\mu(k, R) = 0$. Their minima are $O(\nu)$ close to each other. The $\omega^+ = 0$ branch is below $\mu = 0$; passing this branch causes the first bifurcation at which the trivial solution of (1.4) becomes (linearly) unstable.

Both branches correspond to marginally unstable perturbations (of type (2.1)). From the point of view of the linearized stability theory, it is not important to study the second instability which appears when crossing the $\omega^- = 0$ branch, since this branch is almost everywhere $O(\nu)$ (which is far from the linear point of view) above $\omega^+ = 0$. However, when dealing with the nonlinear problem we will find that the splitting is of crucial importance as long as the distance from criticality is $O(\nu)$ and larger. This is mainly due to the character of the marginally unstable waves associated with these branches.

Before we can continue the analysis, we should specify the meaning of the $o(1)$ term in the resonance condition (2.7). However, now that we know that the neutral stability curve splits into the curves ω^\pm with critical conditions (k^\pm, R^\pm) , it seems

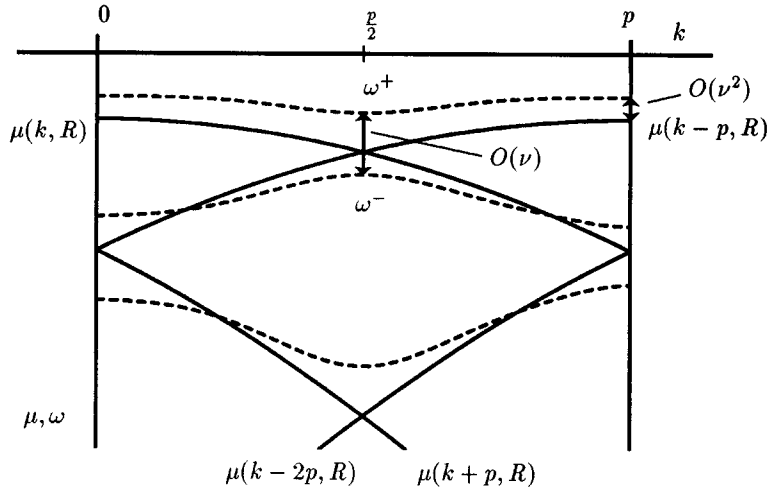


FIG. 2.1. The perturbed and unperturbed dispersion relations as function of k for a fixed value of $R \ll R_c$. The unperturbed dispersion relation (interpreted on a cylinder) is represented as a solid line, while the perturbed dispersion relation is represented by the dotted lines. Note that the distance between the perturbed and unperturbed dispersion relation (by a same value of k) is either $O(\nu)$ or $O(\nu^2)$.

more natural to base the resonance condition on these new critical conditions rather than on the unperturbed conditions (k_c^o, R_c^o) , as is done in (2.7). To achieve this, we first assume that p is given by

$$(2.12) \quad p = -\frac{2k_c^o}{N} + \eta\nu^\beta.$$

Thus, η and β determine the detuning from perfect (but unperturbed) resonance. In [14], a straightforward but cumbersome analysis is then used to show

$$(2.13) \quad p = -\frac{2k^\pm}{N} + O_s(\nu^2, \nu^{2\beta}) \text{ for } \beta > \frac{1}{2},$$

where

$$(2.14) \quad k^\pm = k_c^o + O(\nu^\beta) \text{ for } \frac{1}{2} < \beta < 2,$$

$$(2.15) \quad k^\pm = k_c^o + O(\nu^2) \text{ for } \beta > 2.$$

The case $0 < \beta < \frac{1}{2}$ can be identified with the nonresonant case; there is only one critical condition that plays a role in the weakly nonlinear theory. The other one is too far away to be of importance. The implication of (2.13) is that, for $\frac{1}{2} < \beta < 2$, the system gets “better in resonance.” Herewith we mean that k^\pm satisfies resonance condition (2.7) more accurately than k_c^o does. On the other hand, it can be seen that there is never perfect resonance for the new critical conditions, i.e., we will never reach a situation where k^\pm satisfies resonance condition (2.7) exactly, no matter how close we choose p in a neighborhood of k_c^o . It is even so that if k_c^o is closer than $O(\nu^2)$ to perfect resonance, the system “pushes” the new critical conditions $O_s(\nu^2)$ away from resonance. In other words, the term $\sum F_l \exp(ilpx)$ always has an $O_s(\nu^2)$ detuning with respect to the linear most critical waves $\exp(ik^\pm x) \sum \psi_l^\pm \exp(ilpx)$. From now

on, we will call a problem resonant if p is such that (2.13) is satisfied; in doing so, we have based the resonance condition on k^\pm instead of on k_c^o .

In what follows, we only consider resonant situations for $\beta \geq 1$. The reason for this is that, for $\frac{1}{2} < \beta < 1$, one should take into account the higher-order corrections on (2.13) (which are of order $\nu^{3\beta}, \nu^{4\beta}$, etc.), and one would easily get lost in the subtle transition cases which do not reveal new phenomena.

Remark 2.1. The fact that the graph of the dispersion relation splits into a collection of curves implies that there are gaps in the range of ω . These gaps are essentially caused by the same mechanism as the one which creates the gaps in the spectrum of Hill's equation (see [16], [9]):

$$(2.16) \quad \ddot{x} + (\lambda + \nu F(t))x = 0$$

for $x = x(t)$ and where F is T -periodic and $0 < \nu \ll 1$ (if $F(t) = \cos \omega t$, then (2.16) is the Mathieu equation). The interpretation of the gaps is also similar: if the value of ω is within a gap, there are no solutions of the type (2.1) possible.

Remark 2.2. In the next sections we will use the following results, which can all be derived from a straightforward perturbation analysis (see [14] for the details):

- The solutions that bifurcate at (k^+, R^+) and (k^-, R^-) are associated with the same (up to $O(\nu^2)$ -terms) wavenumber \hat{k} . The relation between k^\pm and \hat{k} is the following:

$$(2.17) \quad k^\pm = k_c^o - \frac{1}{2}\eta\nu^\beta + O_s(\nu^2) \stackrel{\text{def}}{=} \hat{k} + O_s(\nu^2).$$

It follows directly that

$$(2.18) \quad |k^+ - k^-| = O_s(\nu^2).$$

- We have the following relation between the critical values for the bifurcation parameters R^\pm and R_c^o :

$$(2.19) \quad R^+ < R_c^o < R^-,$$

$$(2.20) \quad |R^+ - R^-| = O(\nu).$$

- The N th Fourier mode of the solutions that bifurcate at (k^+, R^+) and (k^-, R^-) (i.e., ψ_N^+ and ψ_N^- ; see (2.1)) is $O(1)$, while all the other Fourier modes are $O(\nu)$ (except of course for ψ_0^+ and ψ_0^- , which are scaled to 1). To be specific:

$$(2.21) \quad \psi_N^\pm = \pm \frac{F_N}{|F_N|} + O(\nu^2).$$

The following relation between the Fourier coefficients can be derived:

$$(2.22) \quad \psi_l^+ \overline{\psi_N^+} = \overline{\psi_{N-l}^+} + O(\nu^2),$$

and the same with an upper index “-”.

3. The structure of the bifurcating waves. In the previous section it was explained that in resonance we actually determine two new critical conditions (k^\pm, R^\pm) , which are both corrections on (k_c^o, R_c^o) . As we are looking at bifurcating solutions from the basic state, at first only (k^+, R^+) is of interest, because $R^+ < R^-$, and the basic state loses its stability at R^+ . However, one should realize that $|R^+ - R^-| = O(\nu)$.

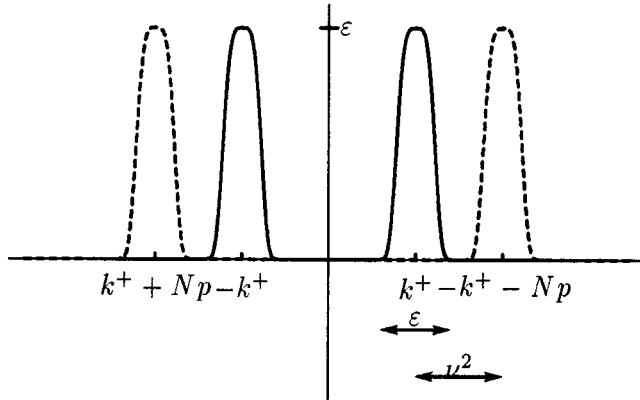


FIG. 3.1. Representation of some modes of the solution Ψ . The solid lines denote the peaks at k^+ and $-k^+$, while the dotted lines denote the “induced” peaks at $k^+ + Np$ and $-k^+ - Np$. The width of the peaks is $O(\varepsilon)$, while the distance between k^+ and $-k^+ - Np$ is $O(\nu^2)$. Thus, for $\varepsilon \gg \nu^2$, the peaks at k^+ and $-k^+ - Np$ (and, of course, at $-k^+$ and $k^+ + Np$, etc.) coincide.

Therefore, if the bifurcation parameter R is increased $O(\nu)$ above R^+ , we must also take into account the second bifurcation point (k^-, R^-) and should consider perturbations of the following form:

$$(3.1) \quad \Psi = \varepsilon \left(A^+(\xi, \tau) e^{ik^+x} \sum \psi_l^+ e^{ilpx} + A^-(\xi, \tau) e^{ik^-x} \sum \psi_l^- e^{ilpx} \right) + \text{c.c.} + \text{h.o.t.}$$

The parameter ε is related to the distance from the critical condition: $R = R^+ + r\varepsilon^2$, and r now plays the role of bifurcation parameter; ξ and τ are slow, rescaled spatial and time coordinates $\xi = \varepsilon x, \tau = \varepsilon^2 t$. These scalings are classical in the theory of amplitude equations: they reflect the fact that with this choice, the nonlinear effects are of the same magnitude as the temporal and spatial developments of the perturbations.

The first part of the solution (3.1) becomes (linearly) unstable at (k^+, R^+) and the second part at (k^-, R^-) . We introduce two amplitude functions, A^+ and A^- , which modulate the waves that bifurcate at (k^+, R^+) and (k^-, R^-) . The aim of the nonlinear theory will be to derive amplitude equations for A^+ and A^- . It should be noted that Ψ (see (3.1)) is the sum of two quasi-periodic functions in x , one with periods k^+ and p and the other with periods k^- and p . The detuning is always of order $O_s(\nu^2)$. In Fourier space, the first part of Ψ can be visualized by means of peaks located at $\pm k^+$ and, “induced” by $\sum F_l e^{ilpx}$, peaks at $\pm k^+ + lp$ for all l (see also Figure 3.1 and [19]). Due to the scaling $\xi = \varepsilon x$, the width of all the peaks is $O(\varepsilon)$. However, in resonance we have

$$(3.2) \quad |(\pm k^+ + lp) - (\mp k^+ + (l - N)p)| = O_s(\nu^2).$$

Thus, if $\varepsilon \gg \nu^2$, the peaks at $(\pm k^+ + lp)$ and $(\mp k^+ + (l - N)p)$ (the latter peaks are related to the c.c.-part) can no longer be distinguished (with respect to ε). In other words, the complex conjugated part of A^+ in Ψ contains modes that are already contained in the part of A^+ itself. The same way of reasoning holds, of course, for the part of Ψ involving A^- . Therefore, for $\varepsilon \gg \nu^2$, we must rewrite (3.1), and it turns out that Ψ becomes periodic in x (instead of quasi-periodic). The detuning that caused the quasi-periodicity of Ψ can be “incorporated” in the ξ -length scale. This reasoning

is clarified as follows. Suppose $\varepsilon \gg \nu^2$, and write $k^\pm = \hat{k} + \sigma^\pm \nu^2$, $p = \hat{p} + \sigma \nu^2$ for some $\sigma^\pm, \sigma = O(1)$ and $\hat{p} = -2\hat{k}/N$. Then, by (3.1),

$$\Psi = \varepsilon \left(e^{i\hat{k}x} e^{i\frac{\sigma^+ \nu^2}{\varepsilon} \xi} \sum A^+ \psi_l^+ e^{il\frac{\sigma^+ \nu^2}{\varepsilon} \xi} e^{il\hat{p}x} + e^{i\hat{k}x} e^{i\frac{\sigma^- \nu^2}{\varepsilon} \xi} \sum A^- \psi_l^- e^{il\frac{\sigma^- \nu^2}{\varepsilon} \xi} e^{il\hat{p}x} \right) + \text{c.c.} \tag{3.3}$$

Note that the evolution on the length scales $\frac{\sigma^\pm \nu^2}{\varepsilon} \xi$ and $\frac{\sigma \nu^2}{\varepsilon} \xi$ is to be considered slow with respect to the evolution on the ξ -scale (because $\varepsilon \gg \nu^2$), and therefore $\psi_l^\pm \exp(il(\sigma^\pm \nu^2/\varepsilon)\xi)$ and $\psi_l^\pm \exp(il(\sigma \nu^2/\varepsilon)\xi)$ can be considered as a constant on the ξ -scale. Taking this, and the relation between the Fourier coefficients ψ_l^+ and ψ_l^- (see (2.21)) into account, we can rewrite (3.3):

$$\begin{aligned} \Psi &= \varepsilon \left(e^{i\hat{k}x} \sum A^+ \psi_l^+ e^{il\frac{\nu^2}{\varepsilon} \xi} e^{il\hat{p}x} + \text{c.c.} + e^{i\hat{k}x} \sum A^- \psi_l^- e^{il\frac{\nu^2}{\varepsilon} \xi} e^{il\hat{p}x} + \text{c.c.} \right) \\ &= \varepsilon \left(e^{i\hat{k}x} \sum \left[A^+ \psi_l^+ + \overline{A^+ \psi_{N-l}^+} \right] e^{il\hat{p}x} + e^{i\hat{k}x} \sum \left[A^- \psi_l^- + \overline{A^- \psi_{N-l}^-} \right] e^{il\hat{p}x} \right) \\ (3.4) \quad &= \varepsilon \left(B^+ e^{i\hat{k}x} \sum \psi_l^+ e^{il\hat{p}x} + B^- e^{i\hat{k}x} \sum \psi_l^- e^{il\hat{p}x} \right) + \text{h.o.t.}, \end{aligned}$$

where $B^+ = A^+ + \overline{\psi_N^+ A^+}$ and $B^- = A^- + \overline{\psi_N^- A^-}$. Note that Ψ has now become a periodic function in x . The detuning between $\exp(i\hat{k}x)$ and $\exp(il\hat{p}x)$ is zero (because $\hat{p} = -2\hat{k}/N$).

Let us look closer at B^+ and B^- . Using (2.21) we find that although the amplitudes A^\pm are allowed to be anywhere in \mathbf{C} , this is not the case for B^\pm :

$$(3.5) \quad B^+ = b^+ e^{-\frac{1}{2}i\gamma + O(\nu)} \text{ for some } b^+ \in \mathbf{R},$$

$$(3.6) \quad B^- = ib^- e^{-\frac{1}{2}i\gamma + O(\nu)} \text{ for some } b^- \in \mathbf{R},$$

and $\gamma = \arg(\psi_N^+)$. Hence, we see that in resonance, and for $\varepsilon \gg \nu^2$, the bifurcating solution (which was arbitrary complex for $\varepsilon \ll \nu^2$) is now split into two parts with amplitudes B^+ and B^- . These amplitudes live on two perpendicular lines in the complex plane, say V^+ and V^- . The angle of V^+ with the positive real axes is related to ψ_N^+ , which is proportional to the N th Fourier mode of the geometrical forcing. From (2.21), it is easy to see that, for the case of real Fourier components F_l , we have $B^+ = \text{Re}(A)$ and $B^- = i \text{Im}(A)$.

Summarizing, we see that in resonance the area of interest is divided into two main parts. The first part is $\varepsilon \ll \nu^2$. In that case the bifurcating solution can be written as

$$(3.7) \quad \Psi = \varepsilon A e^{ik^+ x} \sum \psi_l^+ e^{ilpx} + \text{c.c.} + \text{h.o.t.},$$

which is quasi-periodic in x and becomes linearly unstable at (k^+, R^+) . The second bifurcation point (k^-, R^-) does not play a role yet. The complex conjugated part of the solution cannot be written in the form of the original modes (in other words, the peaks in the Fourier space do not coincide yet), and the splitting of the solution into two parts does not occur. Note that the amplitude A is arbitrary complex.

For $\varepsilon \gg \nu^2$ the solution should be written as (according to the reasoning given in the preceding; see equation (3.4)):

$$(3.8) \quad \Psi = \varepsilon \left(B^+ e^{i\hat{k}x} \sum \psi_l^+ e^{il\hat{p}x} + \varepsilon B^- e^{i\hat{k}x} \sum \psi_l^- e^{il\hat{p}x} \right) + \text{h.o.t.},$$

with $\hat{p} = -2\hat{k}/N$ and \hat{k} the first-order part of k^\pm . This solution is periodic in x . The subtle transition case $\varepsilon = O_s(\nu^2)$ has not been analyzed in detail. In the next section, we will derive amplitude equations for the different regimes in the ε, ν -parameter space, in case of the resonant problem.

4. Weakly nonlinear theory: Derivation of the amplitude equations.

In this section, we consider the cases $\varepsilon \ll \nu^2$ and $\varepsilon \gg \nu^2$ in more detail (recall that ε has been defined by $R = R^+ + r^+\varepsilon^2$). The former case turns out not to be very interesting. However, it can be used to explain the underlying analysis. The details, which are mainly computational, can be found in [14]. Here, we focus on the general aspects of the analysis. Once these aspects are clear, the second case ($\varepsilon \gg \nu^2$) can be handled in analogy, although it turns out that there are some degenerate situations which do not appear in the first case.

4.1. Case 1: $\varepsilon \ll \nu^2$. To start with, one assumes the following expansion of the solution:

$$(4.1) \quad \begin{aligned} \Psi(x, t) = & \varepsilon^2 \Psi^{02} + \varepsilon^3 \Psi^{03} + \dots \\ & + \varepsilon \Psi^{11} + \varepsilon^2 \Psi^{12} + \varepsilon^3 \Psi^{13} + \dots + \text{c.c.} \\ & + \varepsilon^2 \Psi^{22} + \varepsilon^3 \Psi^{23} + \dots + \text{c.c.} \\ & + \varepsilon^3 \Psi^{33} + \dots + \text{c.c.} \\ & + \dots \end{aligned}$$

The functions Ψ^{nm} have the structure $\exp(ink^+x) \sum \psi_l^{nm} \exp(ilpx)$ and are quasi-periodic. For every n, m , and l , the coefficients ψ_l^{nm} can be calculated. After some elaboration, the equations for the coefficients ψ_l^{nm} can be written as

$$(4.2) \quad \mu(nk^+ + lp, R^+) \psi_l^{nm} + \nu \sum_s F_s \psi_{l-s}^{nm} = \mathcal{I}_l^{nm},$$

where μ is again the symbol of the operator \mathcal{L} and \mathcal{I}_l^{nm} is an inhomogeneous term, generated due to nonlinear interaction and due to the introduction of the slow coordinates. For $m > 1$ it contains (depending on m) derivatives of A , with respect to ξ and τ , and linear and nonlinear terms in A . Note that for $n = 1, m = 1$, the coefficients \mathcal{I}_l^{11} are zero for all l , which is a direct result of the linear theory. Hence, Ψ^{11} equals the linear solution multiplied with the amplitude function $A(\xi, \tau)$.

The crucial thing is to now note that the left-hand side (l.h.s.) of (4.2) contains, for $n = 1, m > 1$, and $l = 0$, the term $\mu(k^+, R^+)$, which is $O(\nu)$, while the right-hand side (r.h.s.), \mathcal{I}_0^{1m} , contains terms proportional to ψ_0^{11} (which had been scaled to unity) and is thus $O(1)$ (for instance, for $m = 2$, \mathcal{I}_0^{12} contains terms proportional to $\psi_0^{11} A_\xi$, which is of order ε^2). Thus, there follows that the $O(1)$ -part of

$$(4.3) \quad \mathcal{I}_0^{1m} - \nu \sum_s F_s \psi_{-s}^{1m}$$

should be zero for every m . For $m = 3$, this results in the first order of the amplitude equation for A . The higher-order corrections in ν of this equation can be found by comparing the h.o.t. of (4.2) for $n = 1, m = 3$. The higher-order corrections in ε can also be found from (4.2), but then, for $n = 1, m > 3$. For $n = 1, m = 2$, the $O(1)$ -part of \mathcal{I}_0^{12} is “by construction” zero, which is the result of the rescaling of the variables ξ and τ (this is just like in the classical case; see, for instance, [7]). For $n \neq 1, m$ arbitrary, it should be clear that the l.h.s. of (4.2) is nonzero and $O(1)$ for every l . Thus, in those cases, (4.2) can be solved uniquely for every ψ_l^{nm} .

Summarizing, we can say that for $n = 1, m > 1$ (or in other words, every time the inhomogeneous term can be written in the structure of the linear solution, i.e., as the product of $\exp(ik^+x)$ and a Fourier series with period p), the analysis yields for $l = 0$ an $O(\nu)$ l.h.s. and an $O(1)$ r.h.s. of (4.2), and consequently, by putting the $O(1)$ -r.h.s. equal to zero, one gets the first and higher orders (in ε) of the amplitude equation. The higher-order corrections in ν can be found from (4.2) for a fixed value of m . For the relatively simple case $\varepsilon \ll \nu^2$, the analysis contains no further difficulties, and the above-described process results straightforwardly in the following equation for A :

$$(4.4) \quad A_\tau = r\omega_R A - \frac{1}{2}\omega_{kk} A_{\xi\xi} + 3\beta|A|^2 A,$$

where β is the Landau-coefficient belonging to the equation that one would derive using the model (1.4) with $\nu \equiv 0$. One should not get confused about the coefficient in front of the nonlinear term, which is three times the unperturbed coefficient. In the unperturbed case, the structure of the bifurcating wave is just a modulation of $\exp(ik_c^o x)$. Now, we modulate a wave which reads in first-order $\exp(ik^+x) + \frac{F_N}{|F_N|}\exp(i(k^+ + Np)x) + \text{c.c.}$ and has obviously a different structure. Therefore, there is no reason to expect that the nonlinear coefficient equals the nonlinear coefficient of the unperturbed case.

4.2. Case 2: $\varepsilon \gg \nu^2$. In this case, the structure of the bifurcating waves has been given in (3.8). Recall that this case involves *two* amplitudes: B^+ and B^- . We can no longer assume (4.1) as structure of the solutions, because now, Ψ is periodic instead of quasi-periodic (in x): it is written as the product of a single Fourier mode $\exp(i\hat{k}x)$ and a Fourier series with period \hat{p} , where $\hat{p} = -2\hat{k}/N$. The integer N is going to play an important role. We expand Ψ as follows:

$$(4.5) \quad \Psi = \varepsilon\Psi^{(1)} + \varepsilon^2\Psi^{(2)} + \varepsilon^3\Psi^{(3)} + \dots,$$

where the functions $\Psi^{(n)}$ are Fourier series with coefficients $\psi_l^{(n)}$. Nonlinear interaction between $\Psi^{(1)}$ and itself yields periodic, inhomogeneous terms of $O(\varepsilon^2)$ which contain *quadratic* terms in B^+ and B^- . It should be noted that the terms proportional to $(B^+)^2$ and $(B^-)^2$ live on V^+ , while the terms proportional to B^+B^- live on V^- (V^\pm are defined following (3.5), (3.6)). This is to say that the interaction term consists of two *independent* parts. For general N , this term can be written as the product of a single Fourier-mode $\exp(2i\hat{k}x)$ and a Fourier series with period \hat{p} . Now, a simple analysis shows that for N even, the nonlinear interaction term $\mathcal{N}(\Psi^{(1)}, \Psi^{(1)})$ can be written as a periodic function $\propto \exp(i\hat{k}x) \sum \hat{\psi}_l \exp(il\hat{p}x)$ for some $\hat{\psi}_l$, while for N odd, the term can be written as $\propto \exp(i\hat{k}x) \sum \check{\psi}_l \exp(i(l + \frac{N}{2})\hat{p}x)$ for some $\check{\psi}_l$. Because these terms involve coefficients that live on both V^+ and V^- , it means that the solution for $\Psi^{(2)}$ at the $O(\varepsilon^2)$ -level should also be split into two parts, one that lives on V^+ and one that lives on V^- . For N even, both parts are proportional to $\exp(i\hat{k}x) \sum \psi_l^{(2)} \exp(il\hat{p}x)$ and the coefficients $\psi_l^{(2)}$ (which should actually have an additional upper index “+” and “-”, but for notational convenience, these are omitted) can be determined from the equation

$$(4.6) \quad \mu(\hat{k} + l\hat{p}, \hat{R}) + \sum_s F_s \psi_{l-s}^{(2)} = \mathcal{I}_l^{(2)},$$

where \hat{R} is either R^+ or R^- and $\mathcal{I}_l^{(2)}$ are the coefficients of the interaction term (also actually with upper index + and -). Thus, for $l = 0$, we encounter again the term

$\mu(k^+, R^+)$ in the l.h.s. of (4.6), which is $O(\nu)$, while the corresponding r.h.s. $\mathcal{I}_0^{(2)}$ contains $O(1)$ -terms. Hence, in order to solve (4.6) for $l = 0$, we must have

$$(4.7) \quad \mathcal{I}_0^{(2)} - \sum_s F_s \psi_{-s}^{(2)} = O(\nu),$$

and one should again realize that the l.h.s. of (4.7) contains an $O(1)$ -part which should consequently be zero. Hence, from (4.7) follows again the first order of the amplitude equation (and, of course, the higher-order corrections in ν). Because (4.7) exists with an upper index $+$ and $-$, we get two amplitude equations, one for B^+ and one for B^- ; they contain both quadratic terms. In order to get the higher-order correction in ε , one must proceed in the analysis up to $O(\varepsilon^3)$, i.e., derive the equivalent of (4.6) with upper index (3). Note that the inhomogeneous term \mathcal{I}_l^{nm} can always be split into two independent parts, one living on V^+ and one living on V^- . This is due to the fact that V^+ and V^- are orthogonal.

For N odd, a similar way of reasoning yields that we should pose as structure for $\Psi^{(2)}$ the series $\exp(i\hat{k}x) \sum \psi_l^{(2)} \exp(i(l + \frac{N}{2})\hat{p}x)$ (again, actually with an upper index $+$ and $-$ to distinguish between V^+ and V^-), and we find as equations for the coefficients $\psi_l^{(2)}$ the analogue of (4.6):

$$(4.8) \quad \mu \left(\hat{k} + \left(l + \frac{N}{2} \right) \hat{p}, R^+ \right) \psi_l^{(2)} + \sum_s F_s \psi_{l-s}^{(2)} = \mathcal{I}_l^{(2)},$$

and clearly there is no l such that $\mu(\hat{k} + (l + \frac{N}{2})\hat{p}, R^+)$ is $o(1)$. Hence, (4.8) can be solved uniquely for every l , and the analysis yields no amplitude equation at this level. We must continue the analysis up to $O(\varepsilon^3)$. At that level, it is not difficult to see that the inhomogeneous terms that are generated can be written as $\propto \exp(i\hat{k}x) \sum \hat{\psi}_l \exp(i\hat{p}x)$ for some $\hat{\psi}_l$, which means that the solution for $\Psi^{(3)}$ should have a similar structure. Then, as before, we encounter the term $\mu(\hat{k}, R^+)$ in the equations for the coefficients $\psi_l^{(3)}$ (i.e., (4.6) with the upper index (2) changed to (3)), which is again small, and an analogue reasoning as before leads at this level to the amplitude equations. Of course, these equations do *not* contain quadratic terms but, as usual, *cubic* terms in B^+ and B^- .

The details of the above-described analysis are not difficult but require a precise bookkeeping in order to keep track of all the terms that are going to appear in the amplitude equations for B^+ and B^- (linear, quadratic, cubic terms, derivatives with respect to ξ and τ , etc.). Here, we only give the equations without these details; they can be found in [14]. As explained, we distinguish between N odd and N even.

For N odd, the equations for B^+ and B^- are found to be

$$(4.9) \quad B_\tau^+ = r^+ \omega_R^+ B^+ - \frac{1}{2} \omega_{kk}^+ B_{\xi\xi}^+ + \beta B^+ ((B^+)^2 \psi_N^+ + (B^-)^2 \psi_N^-),$$

$$(4.10) \quad B_\tau^- = (r^+ - \delta) \omega_R^- B^- - \frac{1}{2} \omega_{kk}^- B_{\xi\xi}^- + \beta B^- ((B^+)^2 \psi_N^+ + (B^-)^2 \psi_N^-),$$

where $R - R^+ = r^+ \varepsilon^2, \delta = (R^- - R^+)/\varepsilon^2 = O(\nu/\varepsilon^2)$ and $\omega_R^+ = \frac{\partial \omega^+}{\partial R}(\hat{k}, R^+), \omega_{kk}^+ = \frac{\partial^2 \omega^+}{\partial k^2}(\hat{k}, R^+)$, etc. This coupled set of equations can be rewritten by reintroducing the complex amplitude $A = B^+ + B^-$ and setting $\hat{r} = r^+ - \delta/2$. This yields up to first order:

$$(4.11) \quad A_\tau = \hat{r} \omega_R A - \frac{1}{2} \omega_{kk} A_{\xi\xi} + \beta |A|^2 A + \frac{1}{2} \delta \omega_R \bar{A}.$$

In what follows, we will refer to this equation as the *nonsymmetric Ginzburg–Landau equation*. Note that we actually should have distinguished between ω_R^+ and ω_R^- , etc., but the difference between these expressions disappears in the h.o.t.

For $\nu^2 \ll \varepsilon \ll \sqrt{\nu}$, the coefficient δ is much larger than unity, and we see from (4.10) that B^- is exponentially damped; we return to this point in Remark 4.2.1 below. There are two significant degenerations to consider. The first occurs for $\varepsilon = O(\sqrt{\nu})$, in which case the parameter δ becomes $O(1)$. The second degeneration occurs for $\varepsilon = \sqrt[3]{\nu}$. Then, δ has become of the order of the h.o.t. that we have neglected in the derivation of the amplitude equation. So, for consistency, we should put $\delta \equiv 0$, and what remains is the usual Ginzburg–Landau equation. Thus, the distance between R and the linear stability threshold has become so large that the influence of the p -periodic perturbation $\nu f(x)$ (which was due to the periodic geometry) can be neglected.

For N even, the equations for B^+ and B^- are found to be

$$\begin{aligned}
 (4.12) \quad B^+ &= r^+ \omega_R^+ B^+ - \frac{1}{2} \omega_{kk}^+ B_{\xi\xi}^+ \\
 &+ \beta B^+ \left((B^+)^2 \psi_N^+ + (B^-)^2 \psi_N^- \right) + \frac{\nu}{\varepsilon} (\alpha_1 (B^+)^2 + \alpha_2 (B^-)^2)
 \end{aligned}$$

$$\begin{aligned}
 (4.13) \quad B^- &= (r^+ - \delta) \omega_R^- B^- - \frac{1}{2} \omega_{kk}^- B_{\xi\xi}^- \\
 &+ \beta B^- \left((B^+)^2 \psi_N^+ + (B^-)^2 \psi_N^- \right) + \frac{\nu}{2\varepsilon} (\alpha_1 + \alpha_2) B^+ B^-,
 \end{aligned}$$

where

$$(4.14) \quad \alpha_1 = \frac{2}{\nu} \left(\psi_{\frac{N}{2}}^+ + \psi_N^+ \psi_{-\frac{N}{2}}^+ \right),$$

$$(4.15) \quad \alpha_2 = \frac{2}{\nu} \left(\psi_{\frac{N}{2}}^- + \psi_N^- \psi_{-\frac{N}{2}}^- \right).$$

Note that $\alpha_{1,2} = O(1)$ because $\psi_{\frac{N}{2}}^\pm$ and $\psi_{-\frac{N}{2}}^\pm$ are $O(\nu)$ and $\psi_N^\pm = O(1)$. Note also that we did not write *all* relevant h.o.t. (such as $B_{\xi\xi\xi}^+, B^+ B_\xi^+$, etc.). This is because there is no combination of the magnitudes of ε and ν possible such that these terms become of $O(1)$ -importance. This is not the case for the quadratic and cubic terms in (4.12)–(4.13).

In the case where N is even, there is also a significant degeneration to consider: for $\varepsilon = O_s(\sqrt{\nu})$, the magnitude of the quadratic terms in (4.12) and (4.13) is of order ε and should formally be neglected because (4.10) and (4.13) are only given in first order in ε . Having done that, we can again combine (4.12) and (4.13) to one equation for $A = B^+ + B^-$, and we arrive once more at (4.11).

Remark 4.2.1. From (4.10) and (4.13) one observes that, for $\varepsilon \ll \sqrt{\nu}$ (and, of course, $\varepsilon \gg \nu^2$), the linear coefficient of B^- causes exponential damping of any initial condition. Thus, what remains is only the equation for B^+ (in which we must take $B^- = 0$), which replaces the usual Ginzburg–Landau equation. This equation is either a real Ginzburg–Landau equation (if N is odd) or a real Ginzburg–Landau equation with quadratic terms of order $O(\frac{\nu}{\varepsilon})$. It depends on ε whether the magnitude of these quadratic terms is greater, similar, or smaller than the other terms in (4.12)–(4.13). In either case the dynamics are restricted to V^+ or, in other words, the dynamical situation has become one-dimensional, where it was two-dimensional in the unperturbed case.

In what follows, we focus our attention on the case $\varepsilon = O_s(\sqrt{\nu})$; i.e., we analyze solutions of the nonsymmetric Ginzburg–Landau equation. The remaining cases ($\nu^2 \ll \varepsilon \ll \sqrt{\nu}$) have been analyzed in detail in [14].

5. On the solutions of the nonsymmetric Ginzburg–Landau equation.

5.1. Introduction. In weakly nonlinear theory, one usually fixes ε and denotes the distance above criticality by $r\varepsilon^2$, where r is the bifurcation parameter which can be varied. Changing r means that we change the distance to the minimum of the neutral stability curve. Now the situation is more subtle. First of all, we have two neutral stability curves ω^+ and ω^- . The curve ω^+ is associated with amplitude B^+ and ω^- is associated with B^- . Thus, if we mention “above criticality,” we must specify whether we mean critical conditions belonging to ω^+ or ω^- . As we already know, the distance between the two critical conditions is $O(\nu)$ (and thus fixed). It can lead to ambiguity to use r as bifurcation parameter, because then we can only measure the distance with respect to the minimum of ω^+ and we may overlook the influence of the curve ω^- . To overcome this, we use δ (which measures the relative magnitude of ε^2 with respect to ν) as bifurcation parameter and fix r to 1. Introducing δ still allows us to consider variations in ε because ν is assumed to be fixed. Formally, δ should not become too small because then we may leave the “validity” regime $\varepsilon = O_s(\sqrt{\nu})$. When we use the notation $\delta \ll 1$ and δ small we actually mean that $\varepsilon > \nu^{\frac{1}{2}+t}$ for all $0 < t < 2$ (and a similar line of thought holds for $\delta \gg 1, \delta$ large).

Let us repeat the equations which hold for this case (see (4.11); we applied some cosmetic rescalings, in particular, $A \rightarrow A \exp(i\gamma/2)$, which means that the subspaces V^+ and V^- (see (3.5)–(3.6)) can be replaced by the real and imaginary axis):

$$(5.1) \quad A_\tau = \hat{r}A + A_{\xi\xi} - |A|^2A + \frac{\delta}{2}\bar{A},$$

where $\hat{r} = 1 - \delta/2$ (recall that we fixed r to 1).

Remark 5.1.1. It is well known that (5.1) with $\delta = 0$ admits constant solutions $A = G \exp(i\theta), \theta$ arbitrary. It is immediately clear that these phase-invariant solutions no longer satisfy (5.1) for $\delta \neq 0$; in fact, it is easy to show that the only possible constant solutions are

$$(5.2) \quad A = Ge^{i\theta}, \text{ with } \theta = 0, \pi, \text{ and } G = 1,$$

$$(5.3) \quad A = Ge^{i\theta}, \text{ with } \theta = \frac{\pi}{2}, \frac{3\pi}{2}, \text{ and } G = \sqrt{1 - \delta} \ (\delta < 1).$$

A simple stability analysis (putting $A = G \exp(i\theta) + \hat{a}(\tau) \exp(i\ell\xi)$ and linearizing) shows that (5.2) is always stable and (5.3) is always unstable, as solution of equation (5.1).

The restoration and destruction of the phase-invariance is easily understood if we transform (5.1), using polar coordinates: $\text{Re}(A) = \gamma \cos(\phi), \text{Im}(A) = \gamma \sin(\phi)$. This yields

$$(5.4) \quad \gamma_\tau = \gamma(1 - \gamma^2) + \frac{\delta}{2} (\cos^2 \phi - \sin^2 \phi),$$

$$(5.5) \quad \phi_\tau = -\delta\gamma \sin \phi \cos \phi,$$

and it is immediately clear that $\phi_\tau \rightarrow 0$ for $\delta \rightarrow 0$; phase-invariance is restored.

5.2. Spectral solutions. In this section, we look at simple, space periodic solutions of (5.1). In this section and in the next section, we assume that δ is small so that we can perform an asymptotic analysis in the small parameter δ . Small δ (i.e., large ε) means that we are relatively far above the minima of both curves $\omega^+ = 0$ and $\omega^- = 0$; increasing δ (i.e., decreasing ε) means that we approach the minimum of $\omega^+ = 0$. Before starting the analysis, we consider again the unperturbed case $\delta \equiv 0$. In that case, the equation reduces to the usual Ginzburg–Landau equation, and it is easy to see that there are stationary, space periodic solutions with one Fourier mode only: $A(\xi) = G \exp(ik\xi)$, where $G = g \exp(i\theta)$, $g \in \mathbf{R}$, θ arbitrary, and $k^2 + g^2 = 1$. Thus, the existence criterion is given by $k^2 \leq 1$, and the solutions $G \exp(i(k\xi + \theta))$ form a two-parameter family in the parameters k and θ . We recall a classical result:

- Solutions of the type described above are stable for $|k| < \sqrt{\frac{1}{3}}$ (see [6]); this is known as the Eckhaus stability criterion.

It is obvious that (5.1) no longer admits these pure mode solutions if $\delta \neq 0$. Hence, a natural question arises whenever δ is small: What happens to the stable solutions in the Eckhaus band? This question is the starting point of the subsequent sections.

5.2.1. The structure of the spectral solution. We assume that a general spectral solution of (5.1) can be written as

$$(5.6) \quad A(\xi) = \sum_{n=-\infty}^{\infty} A_n(\tau) e^{ink\xi},$$

where

$$(5.7) \quad A_1 = G = g e^{i\theta} + \text{h.o.t.},$$

$$(5.8) \quad A_{1 \pm n} = O(\delta^n), \quad n \neq 0.$$

This assumption is motivated by the fact that $\lim_{\delta \downarrow 0} A(\xi) = G \exp(ik\xi)$, the periodic solution which satisfies (5.1) for $\delta = 0$.

It is easy to check that assumption (5.6) is invariant under the transformation $A_n \rightarrow A_n \exp(in\theta)$. This means that, without loss of generality, we can take $A_1 \in \mathbf{R}$ (this is to say that $\theta \equiv 0$ and $g = G \in \mathbf{R}$). Substitution of (5.6) into (5.1) leads to an infinite system of coupled ordinary differential equations for $A_n(\tau)$, which can be written as

$$(5.9) \quad \dot{A}_n = (\hat{r} - n^2 k^2) A_n - \sum_{k+l+m=n} A_k A_l \bar{A}_{-m} + \frac{\delta}{2} \bar{A}_{-n}.$$

In what follows, we will write, for notational convenience, B, C, D, \dots instead of A_2, A_3, A_4, \dots . To find the functions B, C , etc., we study the higher-order parts of system (5.9). The $O(\delta)$ part of the solution contains three modes, $k, -k$, and $3k$; they are generated by the nonlinearity and the \bar{A}_{-n} term. Thus, we write

$$(5.10) \quad B(\xi) = \sum_{l=-1,1,3} B_l e^{ilk\xi}.$$

Substituting (5.10) into (5.1) and collecting terms proportional to $\exp(ik\xi)$ lead to an equation for B_1 (recall that $G \in \mathbf{R}$):

$$(5.11) \quad \begin{aligned} 0 &= (1 - k^2 - 2G^2) B_1 - G^2 \bar{B}_1 - \frac{1}{2} G \\ &= -G^2 (B_1 + \bar{B}_1) - \frac{1}{2} G. \end{aligned}$$

The solution of (5.11) can be written as

$$(5.12) \quad B_1 = -\frac{1}{4G} + ib_1, \quad b_1 \text{ arbitrary.}$$

Collecting the terms proportional to $\exp(3ik\xi)$ and $\exp(-ik\xi)$ yields a coupled system of algebraic equations for B_{-1} and B_3 which can easily be solved. We find

$$(5.13) \quad B_{-1} = \frac{G(1 - 9k^2 - 2G^2)}{2(G^4 - (1 - k^2 - 2G^2)(1 - 9k^2 - 2G^2))},$$

$$(5.14) \quad B_3 = \frac{G^3}{2(G^4 - (1 - k^2 - 2G^2)(1 - 9k^2 - 2G^2))}.$$

The analysis can then be continued up to arbitrary order in δ . At δ^n , modes $1 \pm 2n$ are generated while all the existing modes get a correction in their amplitudes. Note that the coefficient of the mode $\exp(ik\xi)$ gets an arbitrary imaginary part at every level of δ . The results can now be summarized as follows. Considering (5.1) with (5.6), the solution reads

$$(5.15) \quad \begin{aligned} A(\xi) &= (G + \delta B_1 + \delta^2 C_1 + \dots)e^{ik\xi+i\theta} + \text{higher harmonics of } O(\delta), \\ B_1 &= -\frac{1}{4G} + ib_1, \quad b_1 \text{ arbitrary,} \\ C_1 &= c_{real} + ic_1, \quad c_1 \text{ arbitrary, } c_{real} = c_{real}(G). \end{aligned}$$

Note that these solutions form a *three-parameter family* (in the parameters k, θ , and b_1 ; c_1 is just the higher-order correction on b_1), whereas in the unperturbed case the solutions formed a *two-parameter family* (phase independent solutions).

To answer the question posed in section 5.2, we must consider the stability of the stationary, space periodic solutions (5.15).

5.3. Stability properties of space periodic solutions. We study the stability of the solution given in (5.15), which we denote by A_p , against a general perturbation ρ . Thus, we substitute

$$(5.16) \quad A(\xi) = A_p(\xi) + \rho(\xi, \tau)$$

and derive an equation for ρ :

$$(5.17) \quad \rho_\tau = \hat{r}\rho + \rho_{\xi\xi} - (2|A_p|^2\rho + A_p^2\bar{\rho}) + \frac{1}{2}\delta\bar{\rho}.$$

For $\delta \equiv 0$, (5.1) reduces to the usual Ginzburg–Landau equation and the periodic solution given in (5.15) reduces to a solution with just one single harmonic. In that case, the stability analysis can easily be performed by substituting $\rho(\xi, \tau) = \tilde{\rho}\exp(ik\xi)$ with $\tilde{\rho} = \int_{-\infty}^{\infty} \rho_l \exp(il\xi) dl$, and one derives a coupled system of ordinary differential equations for $\rho_l(\tau)$ and $\rho_{-l}(\tau)$. The stability of the single mode solution can then be studied by direct linear analysis. For $\delta \neq 0$, this approach doesn't work anymore, which is due to the complex conjugated term in (5.17). If one starts with one single harmonic, all the other harmonics are also generated, and hence, one should write ρ as

$$(5.18) \quad \begin{aligned} \rho(\xi, \tau) &= \sum_{j=-\infty}^{\infty} \rho_j e^{ijk\xi}, \text{ where} \\ \rho_j(\xi, \tau) &= \int_{-\infty}^{\infty} \rho_{j,l}(\tau) e^{il\xi} dl. \end{aligned}$$

After some calculations, we find equations for the coefficients $\rho_{j,l}$ which read

$$(5.19) \quad \begin{aligned} \dot{\rho}_{j,l} = & H_j \rho_{j,l} - (J_2 \bar{\rho}_{-j+2,l} + J_0 \bar{\rho}_{-j,l} + J_4 \bar{\rho}_{-j+4,l}) \\ & - (L_0 \rho_{j,l} + L_2 \rho_{j-2,l} + L_{-2} \rho_{j+2,l}) + \frac{1}{2} \delta \bar{\rho}_{-j,l}, \end{aligned}$$

where the coefficients $H_i, J_i,$ and L_i can be calculated explicitly. They depend on δ and are given in the appendix. It is important to note that (apart from H_j) only $L_0, J_2 = O(1)$; the other coefficients are $O(\delta)$. Equation (5.19) is an infinite system of coupled, linear differential equations, and the eigenvalues of the associated matrix determine the stability properties. We refer to the appendix for the calculation of the relevant eigenvalue, which can be obtained as an asymptotic series in δ . The stability analysis of the single mode solution for $\delta \equiv 0$ gives, of course, the first-order part of the eigenvalue. In the appendix, it is shown that the leading-order and the first-order correction of the eigenvalue is found to be

$$(5.20) \quad \lambda(k, l) = \lambda^{(0)}(k, l) + \delta \lambda^{(1)}(k, l),$$

where

$$(5.21) \quad \begin{aligned} \lambda^{(0)} &= k^2 - l^2 - 1 + \sqrt{(1 - k^2)^2 + 4k^2 l^2}, \\ \lambda^{(1)} &= \frac{\sqrt{(1 - k^2)^2 + 4k^2 l^2} (k^2 - 1 - 2kl)}{\sqrt{(1 - k^2)^2 + 4k^2 l^2} (-2\sqrt{(1 - k^2)^2 + 4k^2 l^2} + 2kl)} \\ (5.22) \quad &- \frac{-((1 - k^2)^2 + 4k^2 l^2) + 2kl(k^2 - 1)}{\sqrt{(1 - k^2)^2 + 4k^2 l^2} (-2\sqrt{(1 - k^2)^2 + 4k^2 l^2} + 2kl)}. \end{aligned}$$

We know a priori that $\lambda(k, 0) = 0$ because we can always construct a perturbation in the direction of the periodic solution which is marginally stable. Furthermore, calculations show that $\lambda^{(1)} > 0$ for all $k, l \neq 0$ and $\lambda^{(1)}(k, 0) = 0$. Thus, the perturbation has a destabilizing effect, and we can immediately conclude that the Eckhaus band cannot become wider. In order to see whether it becomes narrower or not, we expand l around zero, setting $l = \delta l_1$. This yields for $\lambda(k, l)$

$$(5.23) \quad \lambda(k, l) = \delta^2 \left(-1 + \frac{2k^2}{1 - k^2} \right) l_1^2 - \delta^3 \frac{k^2 l_1^2}{(1 - k^2)^2} + \text{h.o.t.},$$

where the $O(\delta^3)$ term in (5.23) comes from the expansion of $\delta \lambda^{(1)}$. Thus, we observe that for k sufficiently far inside the Eckhaus band (that is, $|k| \ll \sqrt{1/3} + O(\delta)$) the $O(\delta^3)$ destabilizing correction can never be bigger than the $O(\delta^2)$ terms, and all solutions with k satisfying $|k| \ll \sqrt{1/3} + O(\delta)$ are stable. What remains to be analyzed are those solutions which are $O(\delta)$ close to the boundary of the Eckhaus band. So, we put

$$(5.24) \quad k = \sqrt{\frac{1}{3}} - k_1 \delta, \quad k_1 > 0$$

and expand (5.23). This yields

$$(5.25) \quad \lambda(k_1, l_1) = l_1^2 \left(-3\sqrt{3}k_1 + \frac{3}{4} \right),$$

and for stability, we must have $\lambda(k_1, l_1) < 0$ for all l_1 . Thus, a necessary condition is $k_1 > \frac{1}{4\sqrt{3}}$, and apparently, for

$$(5.26) \quad |k| < \sqrt{\frac{1}{3}} \left(1 - \frac{\delta}{4} + O(\delta^2) \right),$$

we have stable spectral solutions of the type (5.15). We conclude that the Eckhaus band becomes $O(\delta)$ narrower. Note that the arbitrary coefficient b_1 does not show up in the correction.

The above analysis is restricted to small δ . It seems, however, interesting to look at the dynamics of (5.1) for δ large, within the regime $\varepsilon = O_s(\sqrt{\nu})$. Obviously, this can no longer be done with an asymptotic analysis, and therefore, we turn to numerical simulations. Because we cannot simulate an infinite-dimensional model as given in (5.9), we have to truncate solution (5.6) at some mode, say N . One needs to be careful about the choice of N . On one hand, N must be large enough from a convergence point of view; on the other hand, N should be small to keep the computations within reasonable bounds. We return to the choice of N in section 6.3.

One must immediately realize that truncation has an important consequence for the Eckhaus stability criterion, which states that solutions $A(\xi, \tau) = G \exp(ik\xi)$ are stable for $|k| < \sqrt{1/3}$. It is well known that these waves become unstable by the *side-band mechanism*. This mechanism indicates that perturbations with a very small wave number (i.e., very long waves) are the most unstable ones (see [17]). This observation, however, is a crucial point because in the case that we are dealing with a finite interval, the “most destabilizing” waves may not fit in the interval.

If we want to understand the stability properties of solutions of the truncated system for large δ , we must first understand the consequence of truncation for the case $\delta \equiv 0$. After this, we can study the influence on that situation for δ large. We expect to see somewhere in the dynamics the presence of ω^- and ω^+ , the neutral stability curves.

6. A finite-dimensional model of the nonsymmetric Ginzburg–Landau equation. In this section we fix a wave number and consider the spectral solution (5.6), truncated at mode N . In this finite-dimensional analysis, we denote the wave number with q ; we do this to distinguish this case from the previous section. Note that q determines the length of the finite interval (which is $2\pi/q$, the period of the spectral solution) that we consider. As a start, we consider $\delta = 0$, i.e., we perform a spectral analysis of the usual (symmetric) Ginzburg–Landau equation.

6.1. The symmetric problem. We will look at the spectral solution

$$(6.1) \quad A(\xi) = \sum_{n=-N}^N Z_n e^{inq\xi},$$

and we determine the stability properties of what we denote as a *pure p-mode* (see also [18]). These solutions can be considered as the finite-dimensional equivalents of the solutions $G \exp(ikx)$ that satisfy the usual Ginzburg–Landau equation (i.e., (5.1) with $\delta \equiv 0$) and have the property

$$(6.2) \quad Z_p = \sqrt{1 - p^2 q^2},$$

$$(6.3) \quad Z_n = 0, \quad n \neq p.$$

We immediately observe that the existence criterion is given by $q^2 \leq 1/p^2$. A stability analysis of this solution (putting $Z_p = \sqrt{1 - p^2q^2} + \varepsilon z_p, Z_n = \varepsilon z_n$, and linearizing) leads to

$$(6.4) \quad \dot{z}_p = -2(1 - p^2q^2)z_p,$$

$$(6.5) \quad \begin{pmatrix} \dot{z}_n \\ \dot{z}_{2p-n} \end{pmatrix} = \begin{pmatrix} 1 - n^2q^2 - 2(1 - p^2q^2) & p^2q^2 - 1 \\ p^2q^2 - 1 & 1 - (2p - n)^2q^2 - 2(1 - p^2q^2) \end{pmatrix} \begin{pmatrix} z_n \\ z_{2p-n} \end{pmatrix}.$$

Obviously, the pure p -mode is stable whenever $q^2 < 1/p^2$ (see (6.4); this is exactly the existence criterion) and if the eigenvalues of systems (6.5) have negative real parts for all n . It is now readily seen that the results for a pure p -mode and a pure $-p$ -mode are identical. However, we must be careful. The spectral model is truncated at mode N . Thus, if we consider the stability of the p -mode, the coupling between z_n and z_{2p-n} only exists if n and $2p - n$ are both in the interval $[-N, N]$. If $2p - n \notin [-N, N]$, (6.5) reduces to

$$(6.6) \quad \dot{z}_n = (1 - n^2q^2 - 2(1 - p^2q^2))z_n,$$

and we find stability if $1 - n^2q^2 - 2(1 - p^2q^2) < 0$. Putting things together, we determine a number of critical q_p 's. The minimum of these values is the “ p -discrete analogue” of the Eckhaus criterion. Because this is an important line of thought, we elaborate on the results using $p = 3$. With q_a , we denote the “analytical” stability boundary, obtained by Eckhaus (see [6]): $q_a = \sqrt{1/3}$. Naively, we might expect that the pure 3-mode $Z_3 \exp(3iq\xi)$ becomes unstable if $3q > q_a$; thus $q > \sqrt{1/27}$. However, if we perform the calculations that are mentioned above, it turns out that the 3-mode becomes unstable at $q_3 = \sqrt{1/18}$, and we observe that $q_3 > \sqrt{1/27}$. This latter fact should be no surprise because we already noted that the solutions become unstable by the side-band mechanism. Due to the finite interval (which was a consequence of the truncation) the “most unstable” perturbations, which have a wave number arbitrarily close to zero, do not fit in the interval. Instead, the pure 3-mode only becomes unstable if there is a perturbation possible which fits in the interval. A similar story can be told for the pure 2- and 1-modes, and calculations give the discrete stability boundaries for the modes $q_2 = \sqrt{2/23}$ and $q_1 = \sqrt{2/5}$. Note that both q_1 and q_2 are larger than their analogues on the unbounded domain, i.e., $\frac{1}{2}\sqrt{1/3}$ and $\sqrt{1/3}$.

6.2. The nonsymmetric problem. Let us now look at the influence of δ with respect to these pure p -modes. To give an idea of things that may happen, we analyze the perturbed case on the basis of $N = 3$. This means that we consider a seven-dimensional complex or 14-dimensional real system. Due to the perturbation, a pure p -mode no longer exists for $\delta \neq 0$ except for $p = 0$. From the previous analysis we know that if we consider a pure p -mode for the unperturbed case, the results for the perturbed case are that the $-p, 3p, -3p, 5p$, etc. modes become excited. Thus, for $p = 3$ (and $N = 3$), it means that only the 3- and -3 - modes exist, while for a pure 2-mode, the 2- and -2 modes exist. In case of a pure 1-mode, the 1-, -1 -, 3-, and -3 -modes will be excited for $\delta \neq 0$. The latter case is the most complicated one from a computational point of view, although qualitatively, no new phenomena are encountered. When we talk in what follows about “pure modes,” we actually mean these modes: the perturbed analogues of the pure modes for $\delta = 0$.

Let us first consider the pure 3-mode. The stability properties of this mode can be analyzed explicitly and the analysis will be given in some detail. The results for the 1- and 2-modes can be found in a similar way. To find the amplitudes of the 3- and -3 -modes, we have to solve the following system of equations (we have already taken into account the phase-invariance, which means that we only have to look for real solutions in Z_3 and Z_{-3} ; see section 5.2.1):

$$(6.7) \quad \left(1 - \frac{1}{2}\delta - 9q^2\right) Z_{-3} - (2Z_{-3}^3 + Z_{-3}^2 Z_3) + \frac{\delta}{2} Z_3 = 0,$$

$$(6.8) \quad \left(1 - \frac{1}{2}\delta - 9q^2\right) Z_3 - (2Z_3^3 + Z_3^2 Z_{-3}) + \frac{\delta}{2} Z_{-3} = 0.$$

These equations have eight solutions for Z_3 and Z_{-3} :

$$(6.9) \quad Z_3 = -Z_{-3} = \pm \sqrt{\frac{1 - \delta - 9q^2}{3}},$$

$$(6.10) \quad Z_3 = Z_{-3} = \pm \sqrt{\frac{1 - 9q^2}{3}},$$

$$(6.11) \quad \begin{cases} Z_{-3} &= \pm \frac{1}{4\delta} \left(\sqrt{C_1 + \sqrt{C_2}} \right) (C_1 - \sqrt{C_2}), \\ Z_3 &= \pm \frac{1}{2} \sqrt{C_1 + \sqrt{C_2}}, \end{cases}$$

$$(6.12) \quad \begin{cases} Z_{-3} &= \pm \frac{1}{4\delta} \left(\sqrt{C_1 - \sqrt{C_2}} \right) (\sqrt{C_2} + C_1), \\ Z_3 &= \pm \frac{1}{2} \sqrt{C_1 - \sqrt{C_2}}, \end{cases}$$

where

$$(6.13) \quad C_1 = 2(1 - 9q^2) - \delta,$$

$$(6.14) \quad C_2 = (2(1 - 9q^2) - \delta)^2 - 4\delta^2 = C_1^2 - 4\delta^2.$$

We are actually only interested in those solutions for which $|Z_3| \rightarrow 0$ (or $|Z_{-3}| \rightarrow 0$) for $\delta \downarrow 0$. In that view, one might argue that we can neglect (6.9) and (6.10): for $\delta \downarrow 0$, these solutions (which are both real) tend to solutions in which the 3-mode as well as the -3 -mode are present. However, solution (6.10) turns out to be very important because, despite that it does not *tend* to a pure 3-mode for $\delta \downarrow 0$, it can *bifurcate* into one. The solution (6.9) is indeed neglected. It turns out not to be important for our analysis; besides, it is always unstable. The solutions (6.11) and (6.12) show the before-mentioned behavior: they tend to pure modes for $\delta \downarrow 0$. In Figure 6.1, we have plotted the solutions as function of δ for two specific values of q . This shows that the remaining six solutions are important in our analysis: either they are pure modes or they can bifurcate into pure modes. Figure 6.1 also shows that the role of a pure 3- and -3 -mode can be interchanged. Results, obtained for a pure 3-mode can be directly applied to the pure -3 -mode.

The stability properties of these solutions can easily be studied by direct linear analysis, considering them as solutions of the seven-dimensional complex system. The results are shown in Figures 6.1 and 6.2. These figures should be interpreted as follows. In Figure 6.2, we have plotted curves in the q, δ -plane, which bound the areas of stability of the different types of solutions. We can distinguish between various areas.

First of all, we note that we only consider wave numbers $q < \sqrt{1/18}$ because the pure 3-mode is unstable for $q > \sqrt{1/18}$ and $\delta = 0$. We discuss the behavior of the

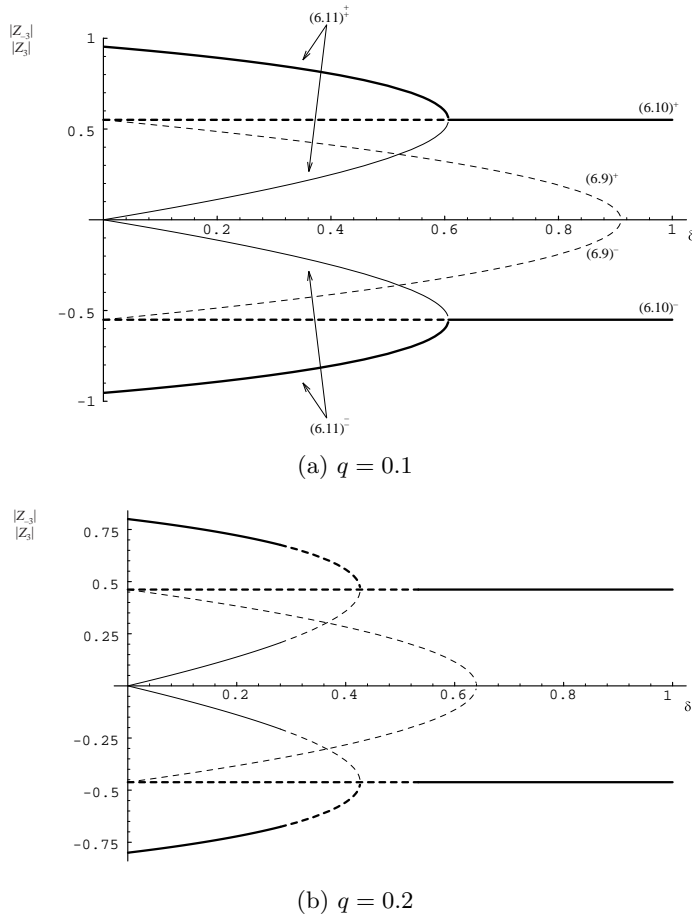


FIG. 6.1. Solutions given by expressions (6.9)–(6.11) for $q = 0.1$ and $q = 0.2$ as function of δ (e.g., $(6.11)^+$ denotes solution (6.11), where one should take the “+” signs). The heavy lines denote the amplitude of the Z_3 component; the thin lines denote the amplitude of the Z_{-3} mode. Stable solutions are solid; unstable solutions are dashed. Solution (6.12) is not drawn; it coincides with 6.11, with the role of Z_3 and Z_{-3} interchanged.

relevant solutions for $q < q^*$ and $q > q^*$, where q^* is defined as the intersection of the three curves, plotted in Figure 6.2. A simple analysis shows that $q^* = 1/6$.

Consider a fixed $q < q^*$, $\delta = 0$, and the pure 3-modes given in (6.11)–(6.12). As indicated in Figure 6.2, solution (6.10) is unstable for these conditions. Then, we increase δ . As a result, the amplitude of the -3 -mode increases, while the amplitude of the 3 -mode decreases. For $\delta = 2/3 - 6q^2$, both amplitudes have become equal and the solutions (6.10)–(6.12) are similar. Increasing δ further, (6.11) and (6.12) “vanish” (that is, they become complex, but due to the phase-invariance, we should only consider real solutions for Z_3 and Z_{-3}) and (6.10) (which is independent of δ) becomes stable. This latter solution exists and remains stable for $\delta \rightarrow \infty$. A specific example for $q = 0.1$ is plotted in Figure 6.1a.

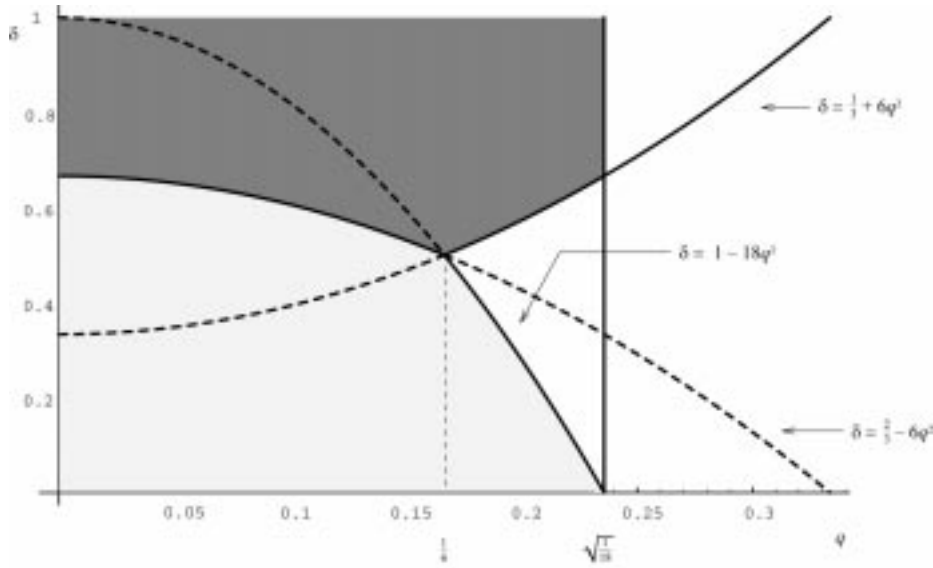


FIG. 6.2. An overview of the stability results for the pure 3-mode in the δ, q -plane. The curves denote where eigenvalues of the various solutions change sign. In the light shaded area, solutions (6.11)–(6.12) are stable; in the dark shaded area, solution (6.10) is stable. To the right of the line $q^2 = 1/18$, there do not exist pure 3-modes. For further explanation, see the text.

For $q > q^*$ the situation is a little bit different. Solutions (6.11) and (6.12) are stable for δ small but become unstable for $\delta = 1 - 18q^2$. For δ larger than $1/3 + 6q^2$, the (real) solution (6.10) is stable but becomes unstable at $1/3 + 6q^2$. We saw that the pure 3-mode solutions (6.11)–(6.12) are “connected” to the real solutions (6.10) by a bifurcation for $q < q^*$. The question is whether this is still the case for $q > q^*$: do the solutions that bifurcate from (6.11) and (6.12) at $\delta = 1 - 18q^2$ match the solutions that bifurcate from (6.10) at $\delta = 1/3 + 6q^2$? From an eigenvalue analysis, we see that at $\delta = 1 - 18q^2$ (that is, coming from below in Figure 6.2) the *real part* of the 0-mode becomes unstable. On the other hand, if we come from above in Figure 6.2, an eigenvalue analysis shows that at $\delta = 1/3 + 6q^2$, the *imaginary part* of the 0-mode becomes unstable and a subsequent bifurcation, where the imaginary part of the -3 and 3 -modes and the real part of the 0-mode become unstable, happens at $\delta = 2(1 + 35q^2)/9$. This indicates that, at least for q close to q^* , both bifurcation scenarios do not match: the pure 3-modes (6.11)–(6.12) are not connected to the real solution (6.10) (see Figure 6.3).

Summarizing, we conclude that in the light shaded area of Figure 6.2, we have a stable, complex solution and an unstable, real solution, while in the dark shaded area, we only have a stable, real solution. In the nonshaded areas, bounded by $\delta = 1 - 18q^2$, $\delta = 1/3 + 6q^2$, and $q^2 = 1/18$, there is no stable solution, with only a 3-mode and a -3 -mode. We conclude from these observations, and this is emphasized, that for all $q < \sqrt{1/18}$ and $\delta > \max(1/3 + 6q^2, 1 - 18q^2)$ there are pure 3-modes which are stable and real.

A similar story can be told for a pure 2-mode. The analysis is omitted; it goes along the same lines as the previous case and the results are qualitatively the same. In Figure 6.4, we have shown the equivalence of Figure 6.2 for the 2-mode.

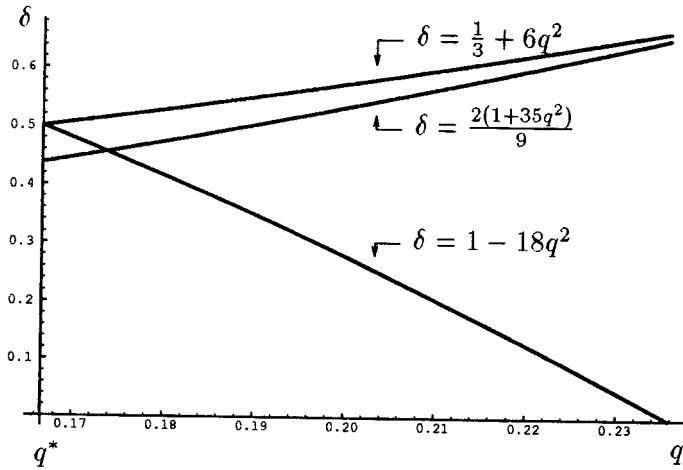


FIG. 6.3. A blow up of Figure 6.2 in the neighborhood of $q_* = 1/6, \delta = 1/2$. At the curves $\delta = 1 - 18q^2$, solution (6.11) bifurcates, at $\delta = 1/3 + 6q^2$, solution (6.10) bifurcates, and a subsequent bifurcation of this solution occurs at $\delta = 2(1 + 35q^2)/9$.

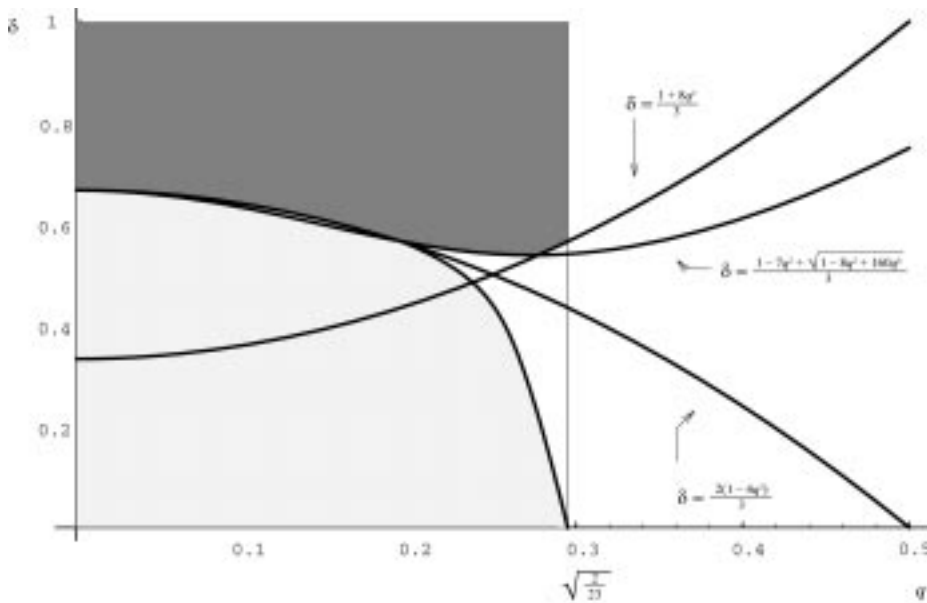


FIG. 6.4. Stability results for the 2-mode. The various lines denote again a change in sign of the eigenvalues of the 2-mode solutions. To the right of the line $q^2 = 2/23$, no pure 2-modes exist.

Then, we study the situation for a pure 1-mode. As already remarked, the equivalent of the pure 1-mode in the finite-dimensional sense is a solution in which $Z_{\pm 1}$ and $Z_{\pm 3}$ are nonzero. In the light of the previous cases (concerning a pure 3- and 2-mode) we expect that, for a fixed q (where q is, of course, smaller than $\sqrt{2/5}$, the stability boundary for a pure 1-mode for $\delta = 0$), there exists a δ for which the total solution becomes real again. Using this information (which means that we can assume $Z_1 = Z_{-1}, Z_3 = Z_{-3}$), it is possible to solve the remaining system of equations

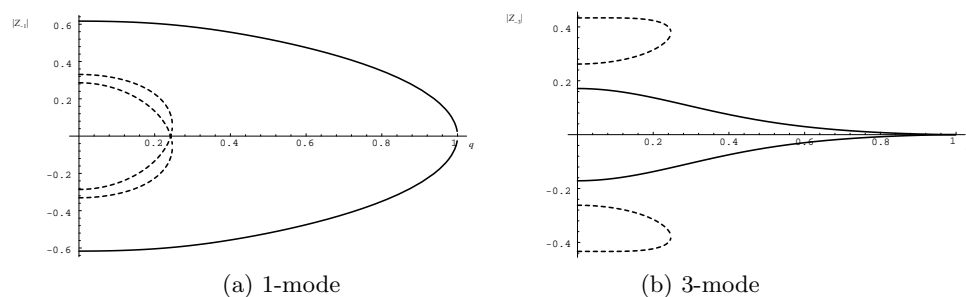


FIG. 6.5. The amplitudes of $Z_{\pm 1}$ and $Z_{\pm 3}$ in the case of a pure 1-mode for δ sufficiently large such that the solution is real, as function of q . Note that the solutions are independent of δ .

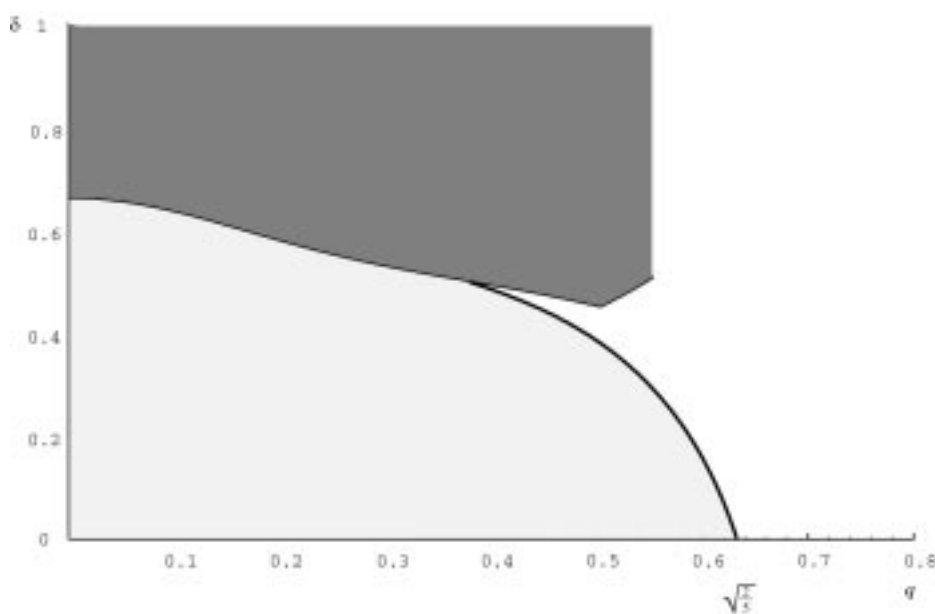


FIG. 6.6. The stability results of the pure 1-mode. In the light shaded area, there are complex, stable solutions; in the dark shaded area, there are only real solutions.

analytically: real solutions, the equivalents of (6.9)–(6.10), can be found and their stability properties can be studied. These results (which are again independent of δ) are shown in Figure 6.5.

Again, stable solutions are represented by solid lines, unstable solutions by dashed lines. Then, we can determine for every q the critical δ for which this solution becomes unstable and construct the equivalents of Figures 6.2 and 6.4 (see Figure 6.6). The bifurcating stable solutions can then numerically be followed for decreasing δ . One of these solutions must, of course, tend to the pure 1-mode for $\delta \rightarrow 0$.

The situation for a pure 0-mode has already been described in Remark 5.1.1. It is easy to see that the amplitude of this mode equals 1 or $\sqrt{1 - \delta}$. As is indicated in Remark 5.1.1, the solution $z_0 = \pm 1$ is stable for all δ , and $z_0 = \pm i\sqrt{1 - \delta}$ is always unstable.

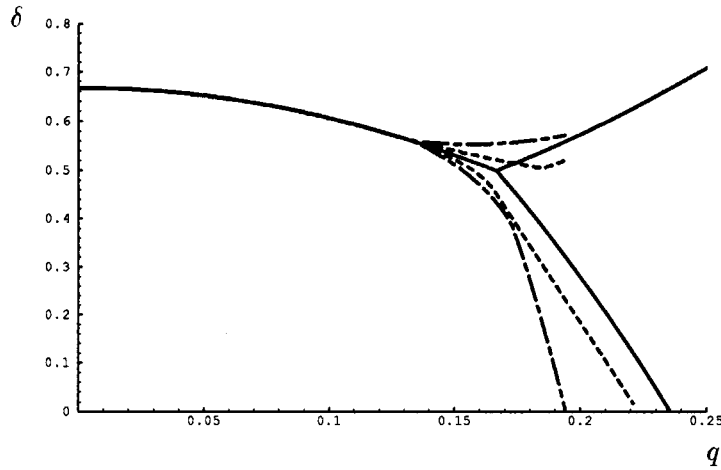


FIG. 6.7. The equivalent of (the relevant) Figure 6.2 for $N = 3$ (the solid lines), $N = 4$ (the dashed lines), and $N = 5$ (the dashed-dotted lines).

An important conclusion that we can draw is that all pure l -mode solutions ($l = 0, \dots, 3$) become real for δ sufficiently large and q smaller than the discrete stability boundary for mode l . This is in agreement with Remark 4.2.1, where we concluded that for ε sufficiently small ($\varepsilon \ll \sqrt{\nu}$), i.e., δ sufficiently large, the amplitude B^- is exponentially damped, and hence, the amplitude is essentially real.

6.3. Considerations on the truncation number. Let us reflect upon the truncation number N . Throughout this section, we took $N = 3$. This choice is not arbitrary. From a computational point of view, N should be as small as possible, but on the other hand, we do not want to make N so small that we exclude interesting behavior. Therefore, we took $N = 3$: it allows us to study the (relatively simple) analogue of pure 2-, 3-modes for the case $\delta \neq 0$ (which contain only ± 2 -, ± 3 -modes) as well as the more complicated analogue of the pure 1-mode, which contains the ± 1 -modes as well as ± 3 -modes. Besides, for the spectral models of the Ginzburg–Landau equation (i.e., the problem under consideration, with $\delta = 0$), it is well known that the norm of the Fourier-modes Z_n of solutions (6.1) exhibits exponential decay. This indicates that the Ginzburg–Landau equation can be approximated by very low-dimensional Galerkin projections. These facts have been proven in [3]. Although the analysis has not been carried out in detail for the nonsymmetric Ginzburg–Landau equation, it is clear that the arguments of [3] can also be applied here since the extra nonsymmetric term $\propto \bar{A}$ has no influence on the essence of the estimates in [3]. Moreover, it has been checked numerically in [1] that the solutions of the Ginzburg–Landau equation on a bounded domain can be approximated by low-dimensional models with high accuracy. Thus, it is expected that the analysis gives similar results: (5.1) can also be approximated by low-dimensional Galerkin projections (on a finite domain). To check this, we considered the 3-mode solutions (6.10)–(6.12) as solutions of the truncated system with $N = 4$ and $N = 5$. Note that (6.10)–(6.12) are explicit solutions of these 18- and 22-dimensional real systems. In Figure 6.7, we have plotted the equivalent of Figure 6.2 for $N = 3, 4$, and 5. We observe that there is a good agreement between the results, which indicates once more that a low-dimensional truncation is justified.

Appendix. The starting point of this appendix is the infinitely coupled set of linear differential equations, given in (5.19) and repeated here:

$$(A.1) \quad \begin{aligned} \dot{\rho}_{j,l} = & H_j \rho_{j,l} - (J_2 \bar{\rho}_{-j+2,l} + J_0 \bar{\rho}_{-j,l} + J_4 \bar{\rho}_{-j+4,l}) \\ & - (L_0 \rho_{j,l} + L_2 \rho_{j-2,l} + L_{-2} \rho_{j+2,l}) + \frac{1}{2} \delta \bar{\rho}_{-j,l} \end{aligned}$$

with

$$(A.2) \quad H_j = 1 - \frac{\delta}{2} - l^2 - j^2 k^2,$$

$$(A.3) \quad J_0 = 2\delta G B_{-1},$$

$$(A.4) \quad J_2 = G^2 + 2\delta B_1 G,$$

$$(A.5) \quad J_4 = 2\delta G B_3,$$

$$(A.6) \quad L_{-2} = 2\delta(G\bar{B}_3 + G B_{-1}),$$

$$(A.7) \quad L_0 = G^2 + 2\delta(G\bar{B}_1 + G B_1),$$

$$(A.8) \quad L_2 = 2\delta(G\bar{B}_{-1} + G B_3).$$

It is important to note that (apart from H_j) only $L_0, J_2 = O(1)$; the other coefficients are $O(\delta)$. The equations for the coefficients $\rho_{j,l}$ can be summarized in one equation as

$$(A.9) \quad \dot{\Theta} = \mathcal{M}\Theta,$$

where Θ is an infinite vector with coefficients $(\dots, \rho_{0,l}, \bar{\rho}_{2,l}, \rho_{1,l}, \bar{\rho}_{1,l}, \rho_{2,l}, \bar{\rho}_{0,l}, \dots)$. In this way, \mathcal{M} has become an infinitely dimensional matrix. Its diagonal contains 2×2 matrices with $O(1)$ entries, the two codiagonals contain 2×2 matrices with $O(\delta)$ entries, etc. The task now is to calculate the eigenvalues of the matrix \mathcal{M} which determines the stability of the zero-solution of (A.1), and thus of A_p . Although the matrix \mathcal{M} is infinite-dimensional, a lot of structure remains, and symbolically, \mathcal{M} can be written as $\mathcal{M} = \mathcal{N}_0 + \delta \mathcal{N}_1 + \delta^2 \mathcal{N}_2 + \dots$, where

$$(A.10) \quad \mathcal{N}_0 = \text{diag}(\mathcal{A}_j^{(0)}),$$

$$(A.11) \quad \mathcal{N}_1 = \text{diag}(\mathcal{B}_*^{(1)}, \mathcal{A}_j^{(1)}, \mathcal{B}^{(1)}),$$

$$(A.12) \quad \mathcal{N}_2 = \text{diag}(\mathcal{C}_*^{(2)}, \mathcal{B}_*^{(2)}, \mathcal{A}_j^{(2)}, \mathcal{B}^{(2)}, \mathcal{C}^{(2)}),$$

for $j \in \mathbf{Z}$. The subscript “*” means adjoint and the superscripts (0), (1), (2) denote the order in δ . All the matrices in (A.10)–(A.12) are 2×2 and can be calculated explicitly using the expansions in δ of H_j, J_j , and L_j ($j = -2, 0, 2, 4$); the relevant parts are as follows:

$$(A.13) \quad A_j^{(0)} = \begin{pmatrix} j - l^2 - j^2 k^2 & G^2 \\ G^2 & 1 - l^2 - (-j + 2)^2 k^2 - G^2 \end{pmatrix},$$

$$(A.14) \quad A_j^{(1)} = \begin{pmatrix} 1/2 & 1/2 - 2ib_1 G \\ 1/2 + 2ib_1 G & 1/2 \end{pmatrix},$$

$$(A.15) \quad B^{(1)} = \begin{pmatrix} 2G\bar{B}_3 + G B_{-1} & 2G B_{-1} + \frac{1}{2} \\ 2\delta G\bar{B}_3 & 2G B_{-1} + G\bar{B}_3 \end{pmatrix}.$$

The matrices with upper index (2) are not needed in the analysis. \mathcal{N}_0 is an infinite-dimensional matrix and its diagonal contains 2×2 matrices. It is important for the subsequent analysis to note that the matrices \mathcal{N}_j are self-adjoint.

The aim is to solve the eigenvalue equation $\mathcal{M}\mathbf{v} = \lambda\mathbf{v}$, where both λ and \mathbf{v} are expanded in δ . The first-order part of the eigenvalue equation leads to the unperturbed eigenvalue $\lambda^{(0)}$ (which is a function of k and l) and the eigenvector $\mathbf{v}^0 = (\dots, 0, v_i^{(0)}, 0, \dots)$, where $v_i^{(0)}$ is the eigenvector belonging to the 2×2 matrix $\mathcal{A}_i^{(0)}$. (For notational convenience, we do not write the subscript “ i ” any longer; the subscripts of $\mathcal{A}^{(j)}$ must be taken from now on relative to “ i ,” i.e., $A^{(j)}$ should be read as $A_i^{(j)}$; $A_1^{(j)}$ should be read as $A_{i+1}^{(j)}$, etc.) The $O(\delta)$ problem can symbolically be written as

$$(A.16) \quad \mathcal{N}_0 \mathbf{v}^1 + \mathcal{N}_1 \mathbf{v}^0 = \lambda^{(0)} \mathbf{v}^1 + \lambda^{(1)} v^{(0)}.$$

Then, we look at the i th and $(i \pm 1)$ th components of the system (recall that we only write subscripts relative to i):

$$(A.17) \quad i\text{th component} : \mathcal{A}^{(1)} v^{(0)} + \mathcal{A}^{(0)} v^{(1)} = \lambda^{(0)} v^{(1)} + \lambda^{(1)} v^{(0)},$$

$$(A.18) \quad (i + 1)\text{th component} : \mathcal{A}_1^{(1)} v_1^{(0)} + \mathcal{B}_*^{(1)} v^{(0)} = \lambda^{(0)} v_1^{(1)},$$

$$(A.19) \quad (i - 1)\text{th component} : \mathcal{A}_{-1}^{(0)} v_{-1}^{(1)} + \mathcal{B}^{(1)} v^{(0)} = \lambda^{(0)} v_{-1}^{(1)},$$

$$(A.20) \quad (i + j)\text{th component} : \mathcal{A}_j^{(0)} v_j^{(1)} = \lambda^{(0)} v_j^{(1)}.$$

From (A.18)–(A.20) we immediately find

$$(A.21) \quad v_1^{(1)} = -(\mathcal{A}_1^{(0)} - \lambda^{(0)})^{-1} \mathcal{B}_*^{(1)} v^{(0)},$$

$$(A.22) \quad v_{-1}^{(1)} = -(\mathcal{A}_{-1}^{(0)} - \lambda^{(0)})^{-1} \mathcal{B}^{(1)} v^{(0)},$$

$$(A.23) \quad v_j^{(1)} = 0 \text{ for } j \neq 0, \pm 1.$$

In principle, $v_j^{(0)}$ can also be calculated (from (A.24)), but this is not needed for the analysis and is thus omitted. In order to find $\lambda^{(1)}$, the first-order correction to the eigenvalue, we make use of the fact that we are dealing with self-adjoint matrices. This means that the eigenvectors are orthogonal (with respect to the Hermitian inner product) and that the image of $(\mathcal{A}^{(0)} - \lambda^{(0)}I)$ is spanned by $w^{(0)}$, where $w^{(0)}$ is the second eigenvector of $\mathcal{A}^{(0)}$. Thus, using (A.17) we find

$$(A.24) \quad (\mathcal{A}^{(1)} - \lambda^{(1)})v^{(0)} = -(\mathcal{A}^{(0)} - \lambda^{(0)})v^{(1)} = \mu w^{(0)}$$

for a certain μ , and taking the inner product on both sides with $v^{(0)}$ gives

$$\langle (\mathcal{A}^{(1)} - \lambda^{(1)})v^{(0)}, v^{(0)} \rangle = 0,$$

and we can calculate $\lambda^{(1)}$. The outcome of the calculations is given in (5.20)–(5.22).

REFERENCES

[1] A. DOELMAN, *Finite dimensional models of the Ginzburg-Landau equation*, Nonlinearity, 4 (1991), pp. 231–250.
 [2] A. DOELMAN, W. ECKHAUS, R. KUSKE, AND R. SCHIELEN, *Pattern formation in systems on spatially periodic domains*, in Nonlinear Dynamics and Pattern Formation in the Natural Environment, A. Doelman and A. van Harten, eds., Longman, UK, 1995, pp. 85–105.
 [3] A. DOELMAN AND E. S. TITI, *Regularity of solutions and the convergence of the Galerkin method in the Ginzburg-Landau equation*, Numer. Funct. Anal. Optim., 14 (1993), pp. 299–321.

- [4] P. M. EAGLES, *A Bénard problem with a perturbed lower wall*, Proc. Roy. Soc. London Ser. A, 371 (1980), pp. 359–379.
- [5] P. M. EAGLES AND K. EAMES, *Taylor vortices between almost cylindrical boundaries*, J. Engrg. Math., 17 (1983), pp. 263–280.
- [6] W. ECKHAUS, *Studies in Nonlinear Stability Theory*, Springer-Verlag, New York, 1965.
- [7] W. ECKHAUS, *On modulation equations of the Ginzburg-Landau type*, in Proc. ICIAM 1991, Washington, DC, SIAM, Philadelphia, 1992, pp. 83–98.
- [8] W. ECKHAUS AND R. KUSKE, *Pattern formation in systems with slowly varying geometry*, SIAM J. Appl. Math., 57 (1997), pp. 112–152.
- [9] A. NAYFEH, *Perturbation Methods*, John Wiley, New York, 1973.
- [10] D. A. S. REES, *The effect of long-wavelength thermal modulations on the onset of convection in an infinite porous layer heated from below*, Phys. Fluids, 2 (1990), pp. 56–62.
- [11] D. A. S. REES AND D. S. RILEY, *Free convection in an undulating saturated porous layer: Resonant wavelength excitation*, J. Fluid Mech., 166 (1986), pp. 503–530.
- [12] D. A. S. REES AND D. S. RILEY, *The effects of boundary imperfections on convection in a saturated porous layer: Near resonant wavelength excitation*, J. Fluid Mech., 199 (1989), pp. 133–154.
- [13] D. N. RIAHI, *Preferred pattern of convection in a porous layer with a spatially nonuniform boundary temperature*, J. Fluid Mech., 246 (1993), pp. 529–543.
- [14] R. SCHIELEN, *Nonlinear Stability Analysis and Pattern Formation in Morphological Models*, Ph.D. thesis, Utrecht University, the Netherlands, 1995.
- [15] R. SCHIELEN, A. DOELMAN, AND H. E. DE SWART, *On the nonlinear dynamics of free bars in straight channels*, J. Fluid Mech., 252 (1993), pp. 325–356.
- [16] J. STOKER, *Nonlinear Vibrations in Mechanical and Electrical Systems*, John Wiley, New York, 1957.
- [17] J. T. STUART AND R. C. DI PRIMA, *The Eckhaus and Benjamin-Feir resonance mechanisms*, Proc. Roy. Soc. London Ser. A, 362 (1978), pp. 27–41.
- [18] L. S. TUCKERMAN AND D. BARKLEY, *Bifurcation analysis of the Eckhaus instability*, Phys. D, 46 (1990), pp. 57–86.
- [19] A. VAN HARTEN, *On the validity of Ginzburg-Landau's equation*, J. Nonlinear Sci., 1 (1991), pp. 397–422.
- [20] I. C. WALTON, *Effects of slow spatial variations on Bénard convection*, Quart. J. Mech. Appl. Math., 35 (1982), pp. 33–48.